Removal of Azo-dyes from wastewater by adsorption on the surface of Graphene Oxide nanosheet: Experimental and Computational approaches

BY

Haris Bin Tanveer

2017-NUST-MS-CS&E-10

A treatise Submitted in the Partial Fulfillment of the Requirement for the Degree of Master of Science (MS)

IN

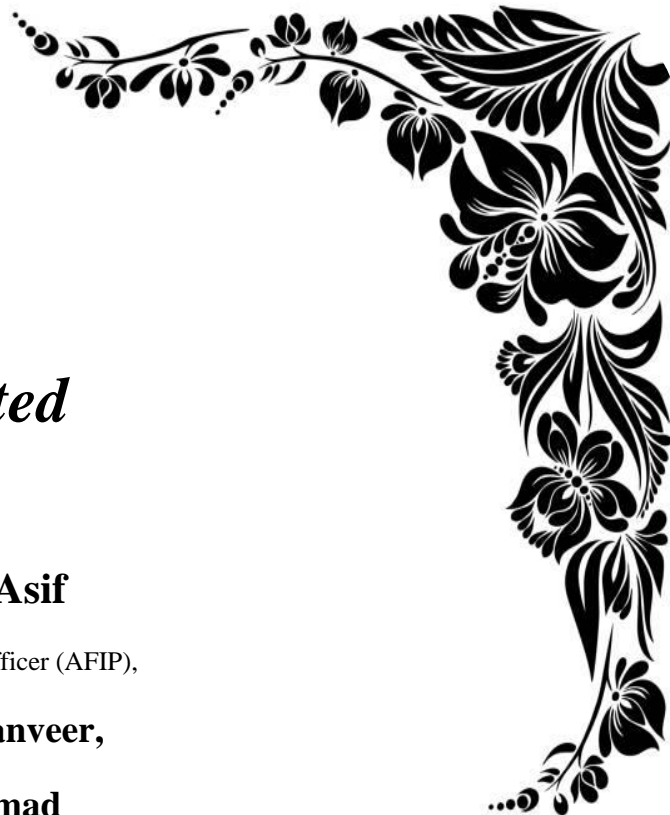## *Computational Science and Engineering*

Supervisor

Dr. Fouzia Malik

Research Centre for Modeling and Simulation (RCMS) National University of Sciences and Technology (NUST)

Islamabad, Pakistan (2019)

Dedicated

To

Tanveer Asif

Senior Scientific Officer (AFIP),

Farzana Tanveer,

Waqas Ahmad
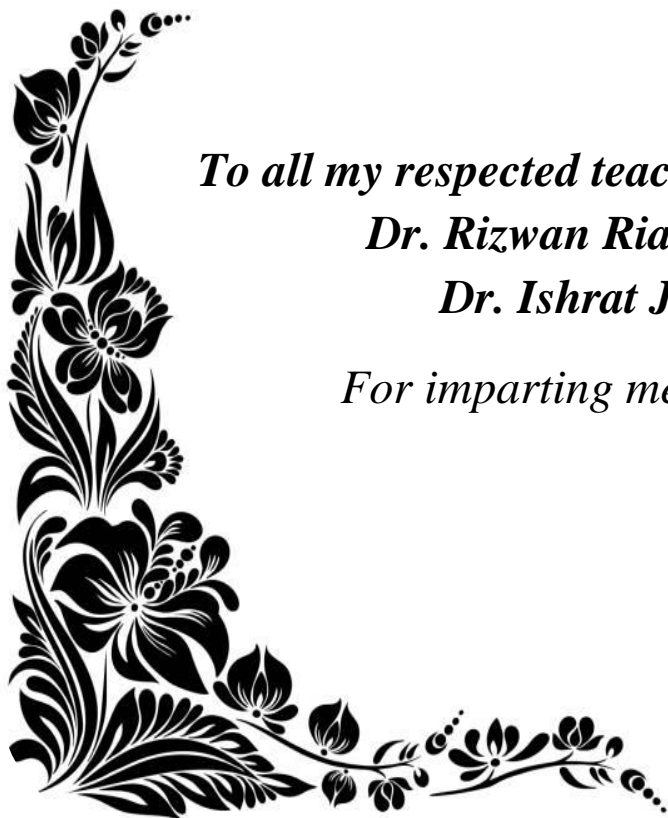
Electrical Engineer, Manager (AWC),

Hasan Ahmad

Senior Software Engineer,

My family

and

To all my respected teachers especially Dr. Fouzia Malik, Dr. Rizwan Riaz (Principle RCMS), and Dr. Ishrat Jabeen (HOD RCMS)

For imparting me with knowledge and skills

Statement of Originality

I hereby proclaim that my thesis work titles "Removal of azo-dyes from wastewater by adsorption on the surface of Graphene oxide Nanosheet by adsorption" is carried out by me under the supervision of Dr. Fouzia Malik at Research Center for Modeling and Simulation (RCMS) in National University of Sciences and Technology (NUST). I solemnly affirm that to the best of my knowledge, this is my original work and it contains no material which has been accepted for the award of other degrees in my name, in any other university. Also, no material previously published or written by any other person has been included in this thesis except where due reference has been made to the previously published work.

Haris Bin Tanveer

MS Computational Science & Engineering

Acknowledgments

List of Contents

List of Abbrebiations

LDA   Local density approximation

GGA   Gradient generalized approximation

DFT   Density functional theory

ADF   Amsterdam density function

UV   Ultra-Violet

Vis   Visible

FT-IR   Fourier Transform Infra-Red

GO   Graphene Oxide

HOMO   Highest occupied molecular orbital

LUMO   Lowest unoccupied molecular orbital

CNT   Carbon nanotube

List of Tables

List of Figures

ABSTRACT

Azo dyes are a coloring agents having wide applications in various industries like paint, textile and paper industries. Azo dyes released as waste materials by textile industries during cleaning process have detrimental impacts on aquatic environment. Now a days heterogenous catalysis and adsorption studies have been gaining much popularity worldwide due to its versatility. Presently heterogenous adsorption mechanism of five novel azo dyes namely, Bis 3,3'-(4,4'-Diazenyldiphenylmethane)-4-chlorobenzaldehyde, Bis 3,3'-(4,4'-Diazenyldiphenylmethane)-p-anisaldehyde, Bis 3,3'-(4,4'-Diazenyldiphenylmethane)-naphthaldehyde, Bis 3,3'-(4,4'-Diazenyldiphenylmethane)-salicylaldehyde, Bis 3,3'-(4,4'-Diazenyldiphenylmethane)-2,4-dihydroxybenzaldehyde with Graphene Oxide (GO) was probed to determine adsorption prosperity on basis of experimental and computational kinetics and thermodynamic parameters. Experimental Langmuir adsorption constant (K_L) determined by UV-Vis spectroscopy was found to be highest for Bis 3,3'-(4,4'-Diazenyldiphenylmethane)-salicylaldehyde *i.e.,* 3.76×10^9 as compared to other four azo-dyes and having more negative free energy value -54.62 kJ/mol. Calculated electronic (E_{HOMO}, E_{LUMO}), kinetic (K_{ad}), and thermodynamic parameters (ΔG, ΔH, and ΔS) based on quantum chemical DFT approach also revealed highest adsorption of Bis 3,3'-(4,4'-Diazenyldiphenylmethane)-salicylaldehyde with Graphene oxide (GO) due to strong deactivating –OH, -CHO group on aromatic ring of azo-dye. Based on quantum chemical findings calculated adsorption constant (K_{ad}) of Bis 3,3'-(4,4'-Diazenyldiphenylmethane)-salicylaldehyde was also highest 1.93×10^{10} and free energy (ΔG) was -58.69 kJ/mol. It was observed that experimental results are complying with computational results. Current research would have tremendous impact in the area of water purification and desalination using Graphene oxide (GO) molecular sieve.

Keywords: Graphene Oxide (GO), Azo dyes, Langmuir adsorption constant (K_L),

Graphical Representation

GRAPHITE	Modified Hummer's Method	Graphene Oxide

ANILINE DERIVATIVE	Coupling Method	AZO DYES
	Alkyl Couplers	

Graphene Oxide **+** AZO DYES → ADSORPTION PROCESS
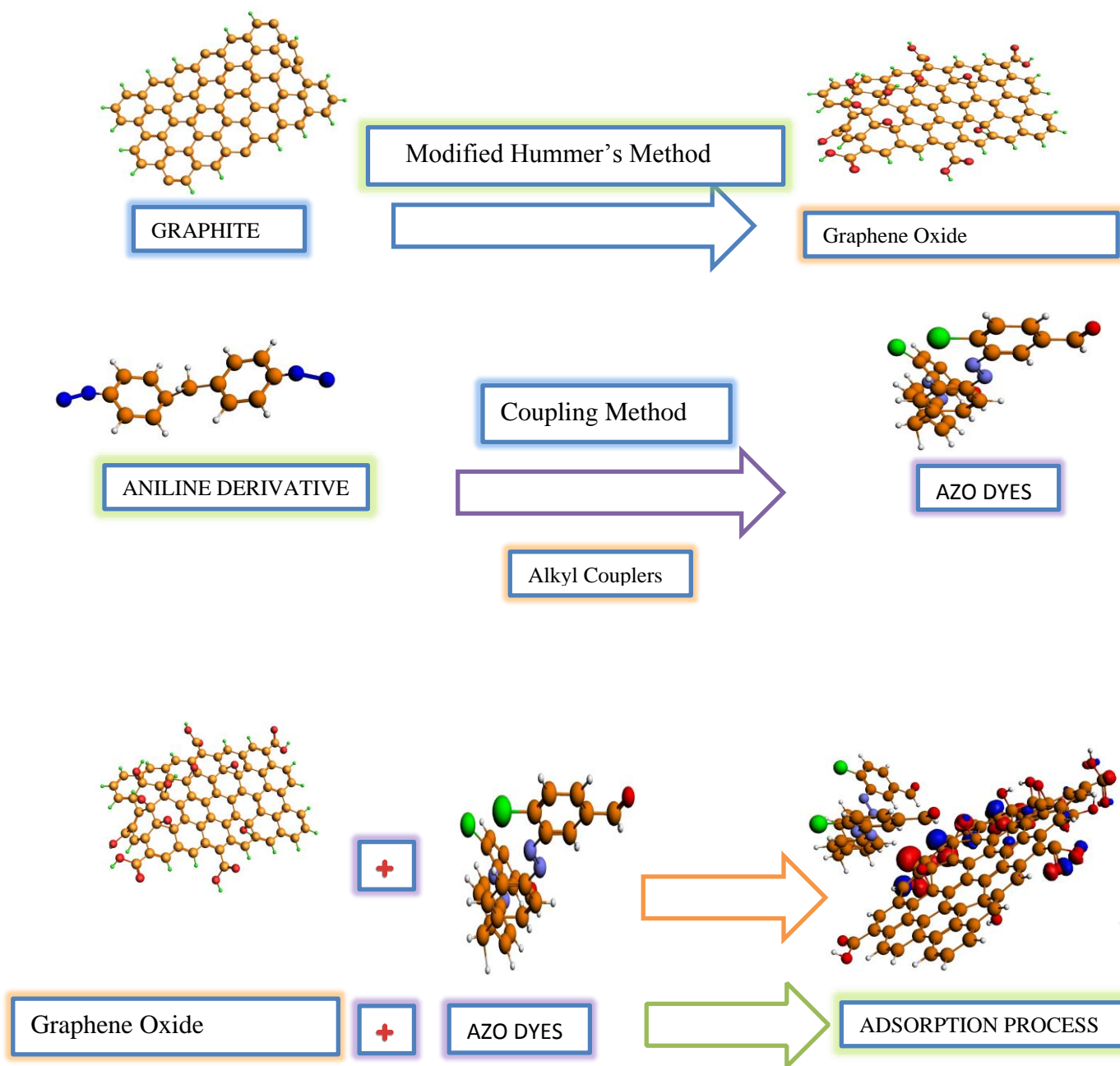
Chapter 1

Introduction

1.1. Background

Drinking water is the most imperative normal asset for a continuation of life, and in view of its worth, it has turned into a prevailing reason for concern. It has gotten increasingly more consideration; the world turned into an obscene with the upkeep and water decontamination. The overpopulation and industrialization i.e., domestic, oil refineries, plastics, food, textile, and paint are harmful origins for the sewage. The ventures of industries bring forth aspects that can possibly adulterate the water. The accommodation community had to set centers for the treatment of the wastewater in an area where these enterprises are set. Azo-dyes are vital compounds that have been well-identified for its broad applications in dye-stuffs, foods, rubbers, pesticides, plastics, and paints. Azo-dyes loaded wastewater released from industries has turned into serious natural trouble for living and aquatic biota. Dyes are organic in nature and they are exceedingly harmful and unfriendly effects on humans, forests, as well as aquatic organisms. Some azo-dyes can cause cancer, skin, eyes, lung, liver, harms; so for safety and lentic life there, removal is necessary[1–5].

1.2 Properties and uses of organic dyes:

The manufacture and utilization of colorants are as old as human history himself. It is an intrinsic craving for humans to look attractive, which deploys the use of colorants in various ways. These colorants can be dyes or pigments depending on the method used. Dyes comprises of two main groups chromophore (part of a molecule which exposes to visible light shows color) and auxochrome (the group of atoms have an ability to alter the intensity of chromophore). Azo-dyes are derived mostly by the coupling of the aryl diazonium salt with a different class of couplers. The azo group contains (N=N) is a chromophore group while other groups like (N $(CH_3)_2$-, C_6H_5 -) attached to chromophore are auxochrome groups. Dyes are synthesized from hydrocarbons such as toluene, anthracene, and benzene. Dyes are being used in paper, artificial plants, textile, pharmaceutical industries, and cosmetics. Dyes used in food colors, drugs, for

coloring silk fiber but they are toxic to humans, forest and animal life. Dyes are useful in chemical industries for analytical research and used as a biological dye[6–8]. Industrial wastewater contains these dyes as pollutants and it is essential to remove azo dyes from water. Chromatography, distillation, evaporation, and coagulation methods used for dye removal from water for its purification but these methods are expensive and are not easy to use. Now a day's adsorption processes by means of nanoparticles used for the subtraction of dye from wastewater because this method is easy to handle. Nanoparticles used as adsorption processes due to their gigantic surface area and efficient adsorption ability. Graphene Oxide and graphene nano-compound were utilized for the removal of many compounds due to their adequate large surface area, porosity, conjugated aromatic structure and high adsorption capability[9–12].

In this analysis, the removal of five novel azo-dyes from wastewater had been studied by using Graphene Oxide as the adsorbent by means of experimental as well as computational approaches. In an experimental approach the adsorption effect of dosage, contact time, sorption studies by UV-Vis spectroscopy were examined. In computational analysis single point, heterogeneous surface interaction through optimization and frequency calculation carried out to study adsorption kinetics and thermodynamics.

1.3 Classification of Dyes

Dyes are divided into several classes based on their chemical nature. The following main categories are

- ❖ Cationic Dyes
- ❖ Anionic Dyes
- ❖ Anthraquinone Dyes
- ❖ Azo dyes

1.3.1 Cationic Dyes

These types of dyes are portrayed as basic because they have a hydroxyl group (OH-) and these dyes can be dissociated into positively charged ions in the aqueous medium. Also, cationic dyes are bright in colors. Cationic dyes are toxic (water-soluble) but their intensity is less than that of anionic dyes. Cationic dyes are used in the dyeing of fabric and leather. For example methylene blue 6B[13-14].
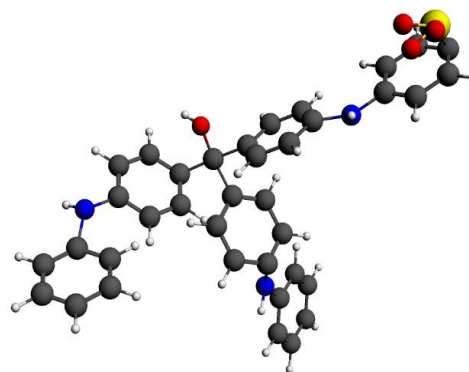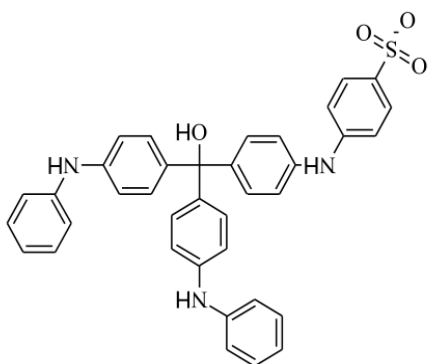
Fig 1.1(a) Cationic Dye Structure (**Methylene Blue)**   **Fig 1.1(b)** Computational Structure

1.3.2 Anionic Dyes

These types of dyes are also known as acidic dyes and they can be dissociated into negatively charged ions in the aqueous medium. Anionic dyes have more reactivity than that of cationic dyes due to the occurrence of reactive groups i.e., azo-group, sulfur, and oxygen (-N=N-, -S=S- & -O=O-). These reactive groups make the binding process easy with the cationic groups. The orange dye is an example of anionic dye[15–17].
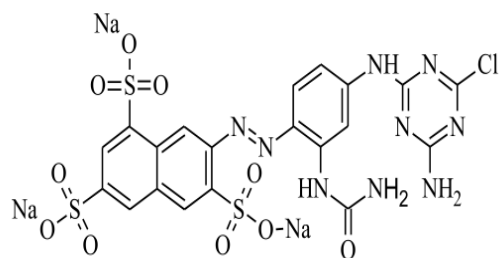
Fig 1.2(a) Anionic Dye Structure (**Orange Dye**)
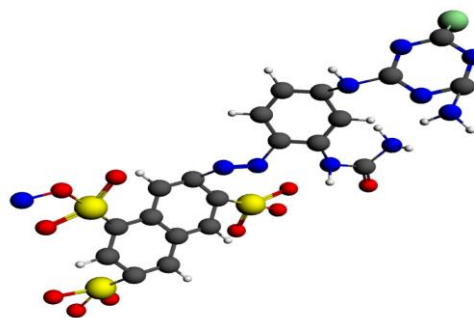
Fig1.2 (b) Computational Structure

1.3.3 Anthraquinone Dyes

These types of dyes are considered as a major class of dyes after azo-dyes. They can be found as natural and man-made dyes. Natural anthraquinone dyes are utilized to dye wool because they are very stable.

Natural anthraquinone dye example is Fusarium oxysporum dye while Alizarin sulfonate is synthetic anthraquinone dye[18–20].
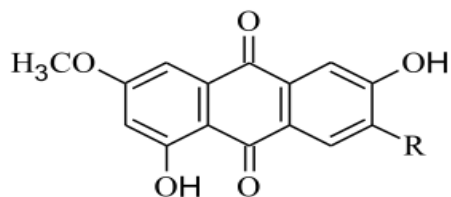
Fig 1.3 (a) Anthraquinone Dye (**Natural Dye**)
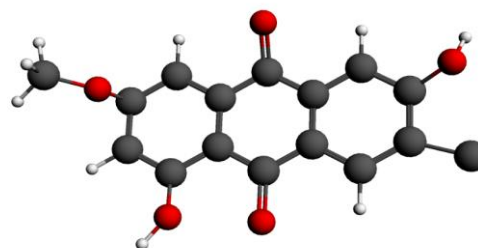
Fig 1.3 (b) Computational Structure
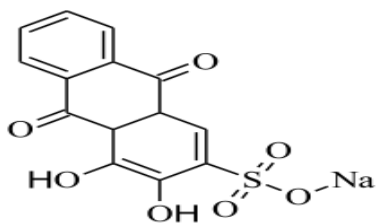
Fig 1.4 (a) Anthraquinone Dye **(Synthetic Dye)**   **Fig 1.4 (b)** Computational Structure
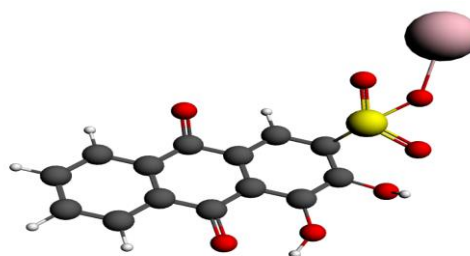
1.3.4 Azo Dyes

These are organic dyes that are synthetically formed, also contain azo (N=N-) group in their structure. About three thousand of azo dyes are utilizing in the paper, food, textile, cosmetics industries. Azo dyes are not easily breakable, when released in an environment they become very toxic pollutants. Azo dyes are very reactive dyes and they evolved as aromatic amines that are highly toxic. Our studies also based on aromatic diamines[21–26].

1.3.5 Methods for removal of Dyes

There are various types of developments that used for water treatment like conventional, emerging and recovery processes [27]. All developed methods; pros and cons are described in Table 1.1.

Table 1.1 Methods for Dye Removal

S.NO	Process	Methods	Merits	Demerits
1.	Conventional Process	Coagulation Flocculation Biodegradation	Easy and less costly	Difficult to get rid of
		Adsorption process	Great surface area capacity	Expensive method
2.	Recovery Process	Separation	High-quality procedure	Bulk samples are not treated
		Ion-Exchange	Safety of adsorbent, useful	Disperse dyes are not treated
3.	Evolving Processes	Innovative oxidation	No need for chemicals	Not liable method
		Biomass	Low cost and selective	pH and salt effected

1.4 Adsorption

Adsorption is a technique where mixture or complexes are adsorbed on the surface of solid. The compound which adsorbs on the surface known as adsorbate while the surface is known as adsorbent this whole phenomenon is called adsorption as shown in figure 1.6
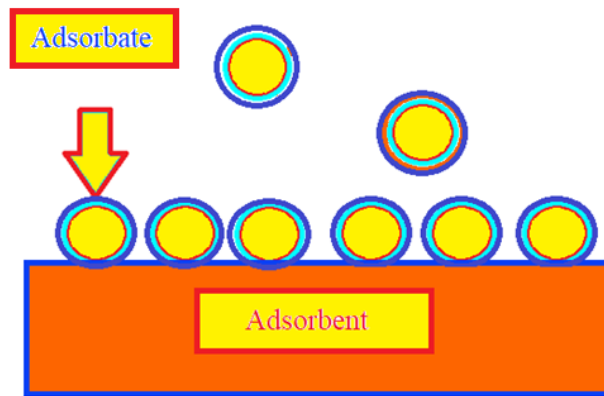
Fig 1.5 Adsorption Process

Adsorption of dyes usually involves four steps:

1. Dissemination of dye through a bulk solution
2. Diffusion of dye molecules via a diffusion layer
3. Dye molecules diffusion into the adsorbent
4. Dye molecules are chemically bound to the adsorbent for the dye removal with a solid adsorbent

Adsorption can be categorized into two types as follows:

1.4.1 Chemisorption

Chemical adsorption is also known as chemisorption. It embraces the development of a strong covalent bond between adsorbent and adsorbate.

The chemisorption and temperature have direct relation i.e., an increase in temperature will cause ascend in chemisorption because energy complications are overwhelmed.

1.4.2 Physical Adsorption

Physical adsorption is also known as physisorption. Physical adsorption comprises weak Vander Waals association between adsorbent and adsorbate.

The physisorption and temperature have inverse relation i.e., an increase in temperature will cause lessening in physical adsorption[28-29].

1.4.3 Factors Affecting Adsorption

The features affecting the rate of adsorption contains the following

1. Initial concentration
2. Adsorbent dosage
3. Contact time
4. Stirring rpm (rotation per minute)
5. Temperature
6. Size & surface area of adsorbent ($\frac{1}{size} \propto surface\ area \propto rate\ of\ adsoprption$).
7. pH

1.4.4 Adsorbent

The material that provides the solid surface for the attachment of dye molecules is called as adsorbent.

The adsorbents mostly used are as follows:

1.4.4.1 Activated Carbon

Activated carbon is a carbon-containing constituent with high surface area and pore size that is acquired from the treatment of raw materials (vegetable source) at elevated temperatures. The warming of raw materials at high temperatures raised the carbon content of the material, quality of carbon content and the pore size. It practically comprises 97% carbon with 3% of other natural substances relying upon the method and raw material utilized for its creation. The permeable surface of activated carbon enables it to

adsorb diverse dyes from the fluid stage that are the main reason for water contamination and used as an effective adsorbent for the subtraction of dangerous dyes.

1.4.4.2 Activated Alumina

The oxide is exploited to prepare porous activated alumina. Activated alumina is formed by warming the hydroxide aluminum oxide and it is activated by the use of acid or steam to expand its surface region and adsorption capacity. Activated alumina has zero-point charge value and due to this specific reason, it is able to adsorb anion dyes from wastewater[30–32].

1.4.4.3 Silica Gel

Silica Gel is poly-porous material with a cross-connecting structure of –Si-O-Si- with siloxane, which is represented by $SiO_2. nH_2O$. Silica-gel behaves as efficient adsorbent because it possesses high surface area due to this reason it is capable for dyes adsorption. Sometimes chemical reagents are added to enhance the adsorption limits of silica-gel, then used to remove harmful dyes from water[33–36].

1.5 Introduction to Nano-particles

Nanoparticles are the smallest particles with a size of fewer than a hundred nanometers (< 100nm). Nanoparticles are a bridge between bulk constituents and atomic structures. Nanoparticles are utilized for adsorption of contaminants from wastewater and nanoparticles have numerous optical applications[37–39]. Nanoparticles have adsorption properties inferable from their little size and they can assimilate harmful dyes from wastewater.

1.6 Categories of Nano-particles

1.6.1 Metallic Nano-particles

Metallic nanoparticles have an immense surface area due to their lesser size. Metallic nanoparticles are stable and their size less than 100nm. Metallic nanoparticles are used for adsorption and drug delivery.

1.6.2 Carbon Nano-particles

1.6.2.1 Carbon Tubes

A carbon nanotube is an allotropic type of carbon, having high quality and electrical conductive properties. Carbon nanotubes have a size ranging from 0.5nm to 3.0nm. Carbon nanotubes are utilized as a transporter for conveying the medication into cell core for curing diseases. Carbon nanotubes (CNTs) have stimulated widespread consideration as a new type of adsorbent due to their outstanding ability for the removal of various inorganic, organic contaminants, and radionuclides from large volumes of wastewater[40].

1.6.2.2 Carbon Nano-particles

Carbon nanoparticles are widely used for adsorption. It is a modified form of graphite powder. Graphite is the source of generation for Reduced graphene and Graphene oxide[41-42]. Carbon nano-particles are used to adsorb dyes. Graphene oxide and reduced graphene oxide detected as planar nano-sheet from X-ray diffraction (XRD).
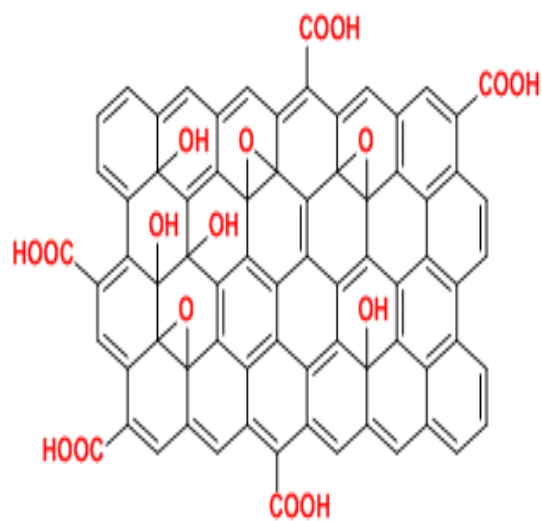
Fig 1.6 (a) Graphene-Oxide   **Fig 1.6 (b)** Computational Structure (GO)
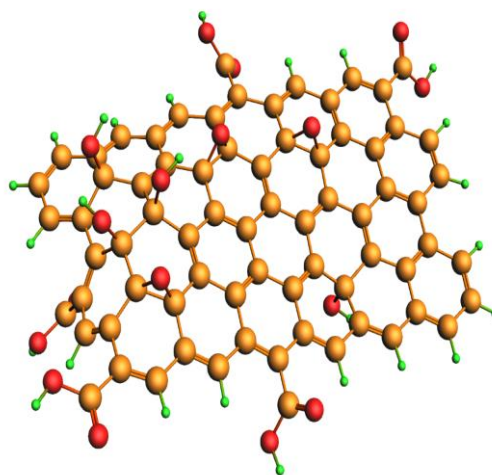
1.7 Properties of Graphene Oxide

Graphene Oxide attracts the researcher aims due to its large quantity of applications in different fields[43–46]. There are following mentioned ample properties:

a) Low manufacturing cost
b) Easy to synthesized
c) Optical properties
d) Versatile electronic properties
e) Highly Conjugated
f) Water dispersible
g) Large surface area
h) Good Mechanical properties
i) Excellent transparency

1.8 Applications of Graphene Oxide Nano-particle

Nanotechnology has advanced importance because of its wide array of applications as nanoparticles. Graphene Oxide is among the nanoparticle that had been used in medical and electric fields. Graphene Oxide is used to absorb radioactive ion from water. It is used for targeted drug delivery in the human body for curing diseases. Now a day researchers are using Graphene Oxide (GO) as a terminal for lithium-ion batteries cells that recharge faster. In Material chemistry, Graphene Oxide (GO) films are being manufactured for removing toxic and hazardous contents from the environment. Graphene oxide sheet is used for treating low-level cancer cells. Graphene Oxide added in the sand to enhance the sand filters to remove the pollutants. Graphene Oxide is the best adsorbent and used for adsorbing dyes from wastewater[47–51].

1.9 UV-Visible Spectroscopy

The absorbance of ultraviolet radiation (200nm - 400nm) and visible radiations (400nm - 800nm) by molecules is associated with the energy gain by an electron and travel from the highest occupied

molecular orbital (HOMO) to lowest unoccupied molecular orbital (LUMO). An absorbance has two characteristics wavelength and molar absorptivity (ε) which is measured by absorbance. The molar absorptivity and absorbance are related by the Beer-Lambert Law as follows:

where,

$$A = \varepsilon \, C \, l \hspace{4cm} 1.1$$

A= *Absorbance*

ϵ =*Molar Absorptivity*

l = *Path length of the cuvette (1 cm)*

Beer-Lambert Law is very useful for quantitative analysis.

1.9.1 UV-Visible Spectroscopy instrumentation

A dual-beam UV-Vis spectrophotometer is used to calculate the quantity of energy absorbed by the standard and by comparing it with the intensity of the beam passing through the molecule at each wavelength of the UV-Vis region, and the result is obtained as a graph of absorbance against wavelength as a spectrum, shown in figure below:
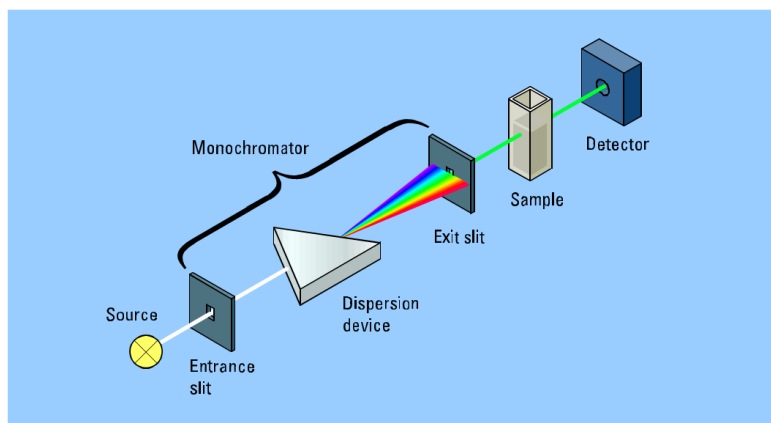
Fig 1.7 UV-Vis Spectroscopy

1.10 Computational Chemistry

Computational chemistry is a modern field of science that utilized Personal Computer (PC) In Computational chemistry various algorithms and equations are used for solving substance issues. Computational chemistry is a reliable contrivance that helps to predict the various properties of the molecules that cannot be possible experimentally. Moreover, it helps to assist the experimental chemistry to figure out the entire novel expedition of chemistry[52-53].

It exploits methods of theoretical chemistry, fused into proficient computer programs, to compute the structures, energies, and properties of molecules *i.e.,* Ab initio method, Semi-empirical method, Density Functional Theory (DFT) methods.

1.10.1 *Ab initio* method

The *ab initio* method, based on Schrödinger equation, is associated to energy of molecule based on wave function (ψ). The wave function is used for determining the electrons distribution from which various properties of molecule are anticipated. The *ab initio* method consumes large amount of time as compared to semi empirical methods.

1.10.2 Semi Empirical method

The semi empirical method is also based on Schrödinger equation. It is a combination of experimental values and theory; the experimental values are parameterized with in Schrodinger equation. The semi empirical method consumes less amount of time as compared to *ab initio* method.

1.10.3 Density Functional Theory (DFT) Methods

Density functional theory methods are very efficient to analyze the properties of molecules by optimizing geometry. DFT methods are based on the Schrödinger equation; where the energy of a particle is a function of electron density while electron density exists as a function of coordinates (x, y & z).

It has the ability to perform various electronic properties like geometry optimization, spectroscopic studies (IR, NMR and so on.), single-point energy calculations, potential energy surfaces, solvation, Hirshfield charge analysis, and time-dependent calculations. Kohn and Sham's theory discussed electrons density and its relationship with energies of a molecule in equation *i.e.,*

$$E = E^V + E^T + E^J + E^{XC}$$ 1.2

Where:

E^V = Potential energy (nuclear-electron attraction and repulsion)

E^T= Kinetic energy

E^J= Electron-electron repulsion energy

E^{XC}= Electron exchange co-relation energy

Due to different approximations in the DFT method, it further distributed in two:

- LDA (Local Density Approximation)
- GGA (Generalized Gradient Approximation)

- *LDA (*Local Density Approximation*)*

  This approximation is a significant class of estimate to the electron co-relations energy in DFT that absolutely relies upon the estimation of electron density at each point in space. This approximation depends on electron density that is uniform in a molecule. In any case, for a particle where the electron density is not uniform, the LDA estimation is not much attractive[54].

- *Gradient Generalized Approximation*

  GGA is an extension approximation of LDA for non-uniform electron density calculations. GGA correlation energy method is best suited to study the interaction between two or more molecules[55].

Chapter 2

State of the Art

In recent years, many researchers paid great attention to the removal of waste; from wastewater by the adsorption method. Wastewater contains many contaminants; among them, the most hazardous are dyeing agents; they pose a greater potential risk to nature. Adsorption observed to be extremely compelling and shabby strategy among all the accessible dye removal strategies. Dyes released as waste by industries can viably isolate by utilizing adsorbent, for example, graphene oxide, metal surfaces, and activated carbon. The adsorption aptitude of dyes depends on the surface area and temperature of an adsorbent. Theoretical and experimental studies revealed that the removal of dyes can be obtained by using less costly, easily available and new adsorbents. Therefore, studies related to searching for proficient and low-cost adsorbents derived from already available material are gaining more importance for the removal of dyes in recent years.

M. Mahdavian *et al.,* (2018) introduced a simplistic approach to synthesize a light preservative nano-particle by means of graphene oxide (GO) and ultra-violet absorber (UVA). DFT studies optimized and observed chemisorption and physisorption between UV absorber and graphene oxide nano-sheet relation. For practical implication, light absorber assimilated to a polyurethane coating and the result revealed that weathering performance improved by three times instability[56].

Aniruddha Molla *et al.,* (2018) reported the adsorption of three colorant dyes on graphene oxide i.e., MB (methylene blue), rhodamine B, and MO (methyl orange). In their research, they used both computational and experimental approaches for adsorption. In the experiment, results showed that adsorption via electrostatic interactions between dye and GO. The positive dyes removal in 15mins was quick and an efficiency rate of 97% for MB and 88% of rhodamine B, respectively while methyl orange, was not adsorbed. In a computational study, Ab initio molecular dynamics were used and the result originates at 2,298 fs for MO and 2,290 fs for MB this demonstrates that MB is more strongly adsorbed on the surface of Graphene oxide nano-sheet (GO)[57].

Lu Gan *et al.,* (2018) synthesized adsorbent by merging alginate hydrogel beads and Graphene oxide. The merging further decreases the pore size of the nanoparticle. The adsorption result was efficient for the subtraction of dyes i.e., azo-dyes, indigo dyes, anthraquinone dyes, and organic dyes[58].

Darian *et al.,* (2018) worked on the removal of the nitrates from water by using graphene nanosheets via MD simulations. Graphene membrane used with different functional groups that helps water permeation and ion rejections[59].

Jafar Azamat *et al.,* (2013) used MoS_2 and Graphene as nanostructure membranes for the removal of arsenic from water. They used 3 types of membranes, with different density to study permeations. The membrane with pores in the center was best suited for the task[60].

Wojciech Konicki *et al.,* (2017) used GO as an adsorbent for the subtraction of two cationic dyes i.e., Basic Yellow 28 and BR 46 [61]. The result of their studies revealed the following aspects:

- Adsorption of these two dyes on graphene oxide was favored at higher pH.
- Adsorption best fit observed was Langmuir isotherm and pseudo-second-order kinetic model.
- Adsorption reaction was a spontaneous and endothermic process.
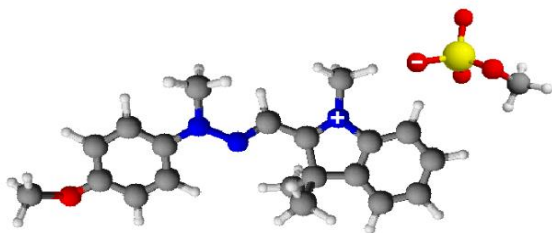
Fig 2.1 Basic Yellow 28   **Fig 2.2** Basic Red 46
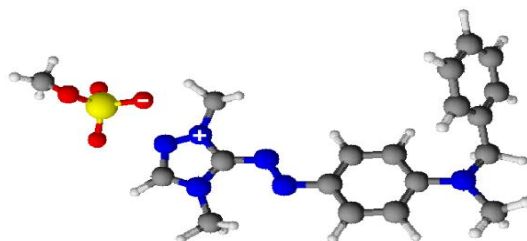
Shiralipour *et al.,* (2017) they adsorbed tartrazine from water by using new adsorbent comprised of cellulose and methyl tri octyl ammonium chloride. The characterization of the new adsorbent was studied by using UV-Vis Spectroscopy, FTIR, X-ray diffraction and SEM while adsorption study was done by batch sorption analysis[62].

Priyakshree Borthakur *et al.,* (2017) synthesized Ag/Graphene Oxide (GO) by the ultra-sonication process. The behavior of various cations, anions on zeta-potential and photocatalytic removal of azo dyes with nanoparticle was studied. The result showed that Ag/GO was efficient for the removal of azo-dyes from aqueous medium[63].

Guilherme Max Dias Ferreira *et al.,* (2017) worked on the removal of Ponceau 4R (PR), Congo Red and Allura Red dyes by adsorbing on multi-walled carbon nanotubes and activated carbon. The characterization was done by the isothermal nano-calorimetry and thermodynamic approaches. The Congo Red dye was maximum adsorbed while the least adsorbed was PR. Thermodynamic parameters depend on surface coverage and enthalpy while entropy was unfavorable[64].
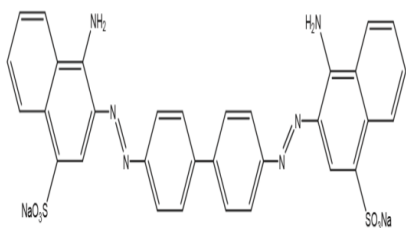
Fig 2.3 Congo Red
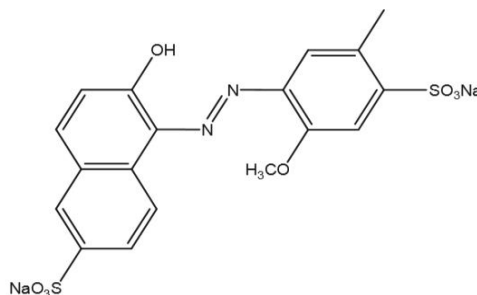
Fig 2.4 Allura Red
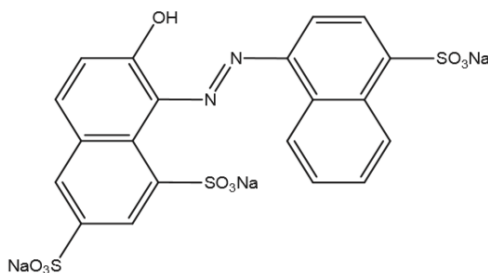
Fig 2.5 Ponceau 4R

Yunchuan Qi *et al.,* (2017) synthesized graphene oxide composite with polysaccharides and worked on the adsorption of organic dyes at its surface. The adsorption characterization was done with FTIR, X-

Ray, TEM, SEM, thermogravimetric analysis and UV-Vis spectroscopy. For analysis of adsorption contact time, effect dosage, pH determined and results showed that PS-GO was efficient adsorbent for both cationic and ionic dyes[65].
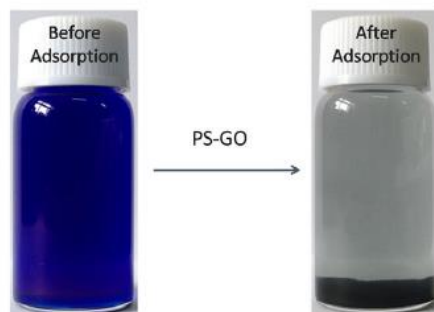
Fig 2.6 Synthesized graphene oxide composite with polysaccharides

Nassar *et al.,* (2016) adsorbed Reactive Black 5 dyes (RB5) on the surface of synthesized Mn_2O_3 nanoparticle. RB5 has versatile used in textile industries and released as waste in the water. The nanoparticle is synthesized by means of the hydrothermal method while its characterization was done by FTIR and X-ray Diffraction[66].

Paszkiewicz *et al.,* (2016) synthesized metallic nanoparticles comprise of Cu and Ag. Characterization analyzed by using X-Ray spectroscopy, TEM, UV-Vis spectroscopy and Zeta potential. The colloidal solution obtained revealed that nanoparticles have anti-fungal and anti0bacterial properties[67].

D. Robati *et al.,* (2015) expressed GO as an adsorbent for the exclusion of two dyes methyl orange and Basic Red 12 (BR-12) from aqueous media. They studied parameters like pH and temperature and optimized these parameters. The results showed that the optimized time-period for the adsorption of dyes was 100mins and pH was 3.0 of aqueous media with the influence of temperature adsorption method of dyes on graphene oxide was endothermic. FTIR was used to study the characterization of GO. Initially, the adsorption rate of the BR 12 increased while methyl orange decreased due to an increase in interaction and repulsion. Resultant values of the adsorption at equilibrium treated with four categories of isotherms i.e., Freundlich, Temkin, Halsey, Langmuir, and Dubin-Rdushkevich isotherms. The finest method was

Langmuir Isotherms due to efficient linear regression which was close to 1 and chi-square values which were between 2.706 and 3.841 ($R^2 = 0.999$ & X^2 is equal to 2.28)[68].
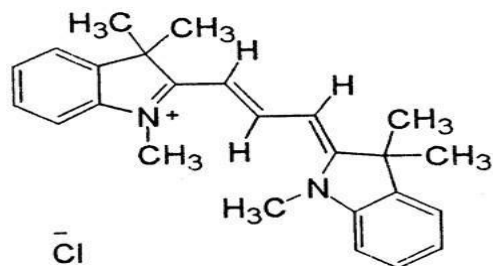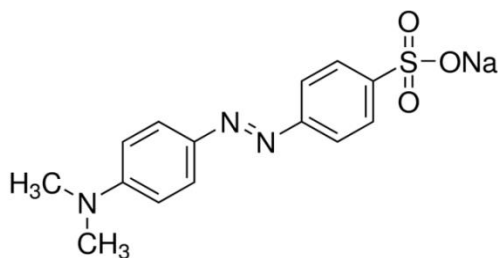
Fig 2.7 Basic Red 12   **Fig 2.8** Methyl orange

Priya Banerjee *et al.,* (2015) calculated the result of azo dyes adsorption on GO nanosheets. The description of GO nano-sheets and its compatibility for adsorption was done by using the AFM, SEM, TEM, and FTIR. The treatment of the wastewater optimized using Artificial Neutral Network (ANN), is used for the elucidation of input, output & for finding patterns of the adsorption. ANN optimization revealed that all the difficulty arises in the process of biosorption. The Temkin isotherms were best compatible with the evaluation of the results. The assay results showed that the dyes completely discharged from wastewater; it can be reuse after adsorption[69].

Animesh Debnath *et al.,* (2015) synthesized nanoparticle of α-Fe_2O_3 by using chemical precipitation method and its characterization was done by X-ray diffraction and EM (Electron microscopy). The nanoparticle of α-Fe_2O_3 used for adsorption of methyl orange dye (MO) from aqueous medium. The result showed that 90% of methyl orange removed by adsorption and Langmuir isotherm model was more appropriate. The kinetic study revealed that adsorption is due to the chemisorption process. Experimental data were analyzed by using ANN (Artificial Neural Network) and showed the removal efficiency rate of dye observed was 95 data points[70].

Ferreira *et al.,* (2015) they used iron nanoparticle covered in lauric acid bilayer for the adsorption of Rifampicin. The characterization of material was done by using zeta potential, FTIR, and TEM. The result showed that Lauric acid bilayer wrapped in iron is efficient adsorber for the Rifampicin[71].

Kassem *et al.,* (2014) synthesized activated charcoal and adsorb tartrazine dyes on its surface. The effect of pH, Dosage, and concentration analyzed. The result revealed that adsorption reaction was exothermic

and adsorption was best at lower pH. The best-fitted model of all was Langmuir isotherm and it shows that activated charcoal efficient adsorber for tartrazine dyes[72].

Xinshan Rong *et al.,* (2014) conveyed adsorption of the congo red dyes from aqueous media by means of Nickel Oxide Graphene Nanosheets (NGNS). For this determination, they organized the synthesis of the NGNS and studied properties by UV-Vis spectroscopy, X-ray diffraction, Thermogravimetric, transmission electron microscopy, High-resolution transmission electron microscopy, RAMAN spectroscopy. The result showed that Congo red adsorbed on NGNS with a proficiency of 99.56% and pseudo kinetic second order and equilibrium fact all followed the Redlich model. Their study observed that the NGNS had the potential to deal with the Congo red dye in wastewater[73].
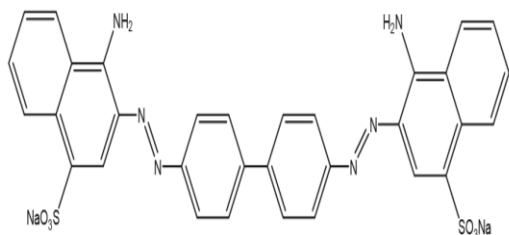
Fig 2.9 Congo Red dyes   **Fig 2.10** NiO_2/graphene oxide nano-sheet
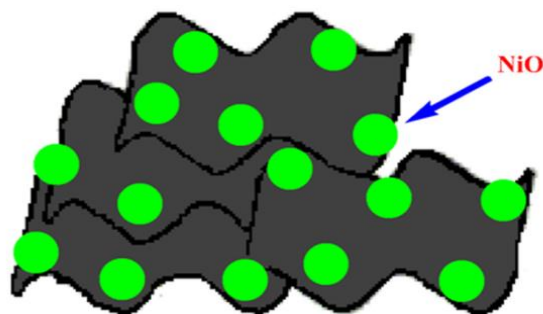
Klett C *et al.,* (2014) synthesized Nickel doped zinc oxide nanoparticles used for adsorption of Methyl orange and tartrazine dye from water. The adsorption depends upon the initial concentration, pH, temperature, and dosage. Adsorption kinetic study showed that pseudo-second-order and Temkin and Freundlich isotherm were best fit for adsorption[74].

Ali Fakhri *et al*., (2013) conveyed adsorption of the aniline from aqueous media by means of graphene Oxide (GO). Analyses of adsorbent dosage effect and contact time analyzed, while contact time data best fitted to the Langmuir isotherm. The thermodynamic study showed an endothermic and spontaneous process[75].

Zhang *et al.,* (2013) studied the adsorption of Methyl Blue dye on metallic nanoparticle of zinc. Zinc oxide nanoparticles have a high capacity rate to adsorb MB on its surface. This metallic based adsorption

does not dependent on pH and temperature. The adsorption occurred because of an ionic bond between adsorbent and adsorbate. Temkin isotherm was best suitable for MB adsorption[76].

Ghaedi *et al.,* (2013) modified activated carbon by the coating of tin sulfide nanoparticle (SnS-NP-AC) and used to adsorb the Reactive orange 12 dye. The characterization of this specific nanoparticle analyzes by using SEM, X-ray diffraction and UV-Vis spectroscopy. The adsorption efficiency analyzed by means of all possible factors affecting the adsorption. The kinetic and thermodynamic study showed that pseudo-second-order and endothermic processes between the nanoparticle and Reactive Orange dye[77].

Wang *et al.,* (2012) worked on adsorption of Reactive Blue 194 dye from aqueous medium by means of Fe_2O_4 particles. Fe_2O_4 particles not efficient adsorber in aqueous media so they worked to improve quality by HCl assisted sonication. The efficiency rate of adsorbing was 90% but it reached equilibrium at less than 40mins. Langmuir isotherm was appropriate for this adsorption[78].

Machado *et al.,* (2011) studied the removal of Reactive Red M-2BE dye from wastewater by means of carbon nanotubes and activated carbon as adsorbent. The nano-particle characterization done by IR, SEM, and adsorption/desorption isotherms. The adsorption efficiency analyzed by means of pH, shaking speed, contact time and temperature[79].

Kanawade *et al.,* (2010) used Sugar cane bagasse ash as an adsorbent for Acid Orange-II dye. Batch mode sorption applied to study the adsorption process. Their research confirmed that increasing the removal of dye occurred by decreasing the flow rate, increasing the bed height[80].

2.1 GAP Identifications:

Modern researchers working on synthesized newly azo-dyes and used them as colorants in textile, marble, and paper industries. Five novel azo-dyes are synthesized in current research similar methodology were utilized for syntheses but different products obtained as a result. Industries released a lot of quantity of azo-dyes as waste and contaminate the water. Some azo-dyes are reported as carcinogenic so their removal is necessary whether it is carcinogenic or not to save water. Now a day researchers also considered a number of materials for the adsorption of azo-dyes using computationally and experimental approaches. There are not any computational studies were done yet but it can provide the widespread computational detail for explaining the kinetic of adsorption behavior, Hirshfield charge analysis, thermodynamic parameters, and other parameters; in this research, these parameters were determined. Adsorption of the "Parallel" configuration of azo-dyes with Graphene Oxide has been to explore the possible binding site for stable adsorption. Indeed, some material researchers used metal surfaces and activated carbon to study the possible adsorption of azo-dyes on their surfaces but the rate of adsorption is low as compared to graphene oxide nano-sheet. Thermodynamics and kinetic behavior for adsorption study were not explored in detail. Variation of complex energy with distance 3.5 Å between the double bond of benzene in azo dyes with epoxide group on Graphene Oxide was not studied yet. The current study immersed to grow a better knowledge of the adsorption behavior of novel azo dyes on Graphene Oxide (GO). Distance delivers a pivotal part in the adsorption studies and assisted significantly toward adsorption constant, free energy, enthalpy, entropy, Hirshfield charge analysis, and adsorption energy. HOMO and LUMO energy orbital further describes the interaction between azo-dyes and GO. Potential energy surface contingent the stability and binding affluence between adsorbate and adsorbents.

2.2 Problem Statement:

Azo-dyes catalytic reduction by skin microflora, liver, and intestinal enzymes produces amines that are reported carcinogenic for humans and animals as shown in Figure 2.11. Dyes released as waste but precaution measures are major concerns for a sustainable environment that had not been investigated and addressed. The removal through cost-effective adsorbent to adsorb azo-dyes is a hot topic of interest.
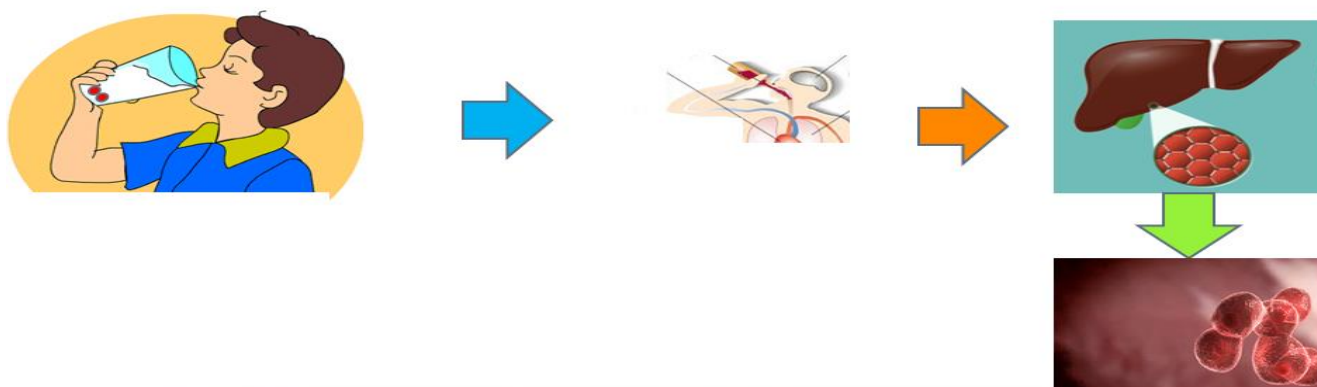
Fig 2.11 Carcinogenicity of dye in Pictorial Representation

2.3 Preface and Significance of current research

Currently, in the modern era, nano-particles are widely being used for adsorption purposes. Many researchers adsorb different dyes on the surface of adsorbent but very few theoretical studies have been reported to explore the adsorption behavior of dyes using both experimental and computational methods. Current research desire to investigate the adsorption of newly synthesized organic azo dyes on the surface of Graphene Oxide(GO) nano-sheet employing both experimental UV-Vis spectroscopy and computational quantum chemical approaches which have not been explored till yet for adsorption of five new synthesized dyes on Graphene Oxide are not in limelight but current research contains both aspects. The names of five novel azo dyes are shown in Table 2.1.

Table 2.1 Five novel azo-dyes

IUPAC Names	Abbreviation Names	Structure
Bis 3,3'-(4,4'-Diazenyldiphenylmethane)-4-chlorobenzaldehyde	(HT 1-1)	
Bis 3,3'-(4,4'-Diazenyldiphenylmethane)-p-anisaldehyde	(HT 1-2)	
Bis 3,3'-(4,4'-Diazenyldiphenylmethane)-naphthaldehyde	(HT 1-3)	
Bis 3,3'-(4,4'-Diazenyldiphenylmethane)-salicylald-ehyde	(HT 1-4)	
Bis 3,3'-(4,4'-Diazenyldiphenylmethane)-2,4-dihydroxybenzaldehyde	(HT 1-5)	

Azo-dyes and Graphene Oxide interaction were analyzed for surface adsorption kinetics, thermodynamic, Langmuir isotherm, the effect of dosage and contact time gives adsorption constant (K_{ad}) and free energy (ΔG) calculated and validate from computationally calculated Gibb's free energy. Azo dyes with maximum K_{ad} and most negative ΔG show the most efficient adsorption.

2.4 Objectives

The main objectives of the current research are as follows:

1. To identify the nature of Azo dyes adsorption on Graphene oxide (GO) molecular sieves physisorption or chemisorption.
2. To investigate the strength of Azo dyes adsorption based on kinetic and thermodynamic parameters.
3. Relation of experimental findings by computational results to visualize molecular level adsorption mechanism.

Chapter 3

Materials and Methods

Chapter 3

SECTION-I : EXPERIMENTAL-MATERIALS AND METHODS

The detail specifications of materials and experimental strategy meant for the proposed adsorption of novel azo dyes on the surface of the Graphene Oxide nano-sheet were clarifying in this chapter. It also incorporates testing instrumentation conditions and preparation of samples as per standards.

3.1 Apparatus and Chemicals

The apparatus including volumetric flasks, measuring cylinders, funnels, measuring flasks, syringe filter, pipette, aluminum foil, Petri dishes, magnetic bar, beakers, china dishes, test tubes, glass rod, and micropipette was used during research work. Following are the further chemicals of analytical grade which were used in the present research are depicted in Table 3.1

Table 3.1 Chemicals name along with their company name

Sr.No	Name of chemical	Company
01	HNO_3 65 %	Merck Germany
02	HCl 37 %	Merck Germany
03	Sulphuric acid 95-98 %	Merck Germany
04	Graphite powder	Sigma Aldrich
05	Potassium permanganate	BDH England
06	Hydrogen peroxide 35 %	Scharlau
07	Deionized Water	Sigma Aldrich
08	Aniline derivatives	Merck Germany
09	Dimethyl sulfoxide 99.9 %	VWR Chemicals

3.2 Methods for Preparation Graphene Oxide Nano-particles

3.2.1 Modified Hummer's Method

In this method concentrated nitric acid, sulfuric acid and potassium permanganate were utilized to synthesize Graphene Oxide from graphite powder. Modified Hummer's Method is considered to be the safer method and it reduced preparation time from 7 days to 3 days. The suspension was diluted with water and hydrogen peroxide (H_2O_2) was added to eradicate manganese from the dispersion.

3.2.1.1 Synthesis of Expanded Graphite

The following procedure has been adopted for the synthesis of expanded graphite. Added 30 mL of concentrated sulfuric acid in 250mL beaker and placed it on a hot plate for stirring. Added 30mL of concentrated nitric acid dropwise in a medium. The 15 grams of graphite were added into this medium; covered the beaker via lid and let solution soaked for 3 days. After three days, transferred this entire mixture into 200mL deionized water in 500mL beaker and leveled it up to the mark. The intercalation of graphite occurs which is known as expanded graphite. Expended graphite has low density due to this reason the mixture was centrifuged for 30mins. Two-layer were generated after centrifugation the upper layer was decanted while the lower layer of black precipitate was warmed in the oven at 70°C for 3-4 hours. After heating the intercalation of graphite was obtained, it was highly hydrophilic and effectively be oxidized.
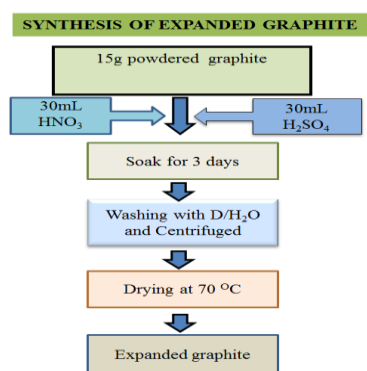
Fig 3.1 Schematic depiction of synthesis of expanded graphite

3.2.1.2 Synthesis of Graphene Oxide

Graphene Oxide nano-sheet was synthesized using an improved Hummer's method; it is based on chemical exfoliation. Oxidation of extended graphite done by taking 75mL of concentrated sulfuric acid in 250mL beaker with continuous stirring for 20mins, during stirring process added 4 grams of expanded graphite in three intervals. The solution placed in an ice bath and proceeded with the stirring.

Added 12 grams of potassium permanganate (**KMnO$_4$**) in solution.

Reaction:

$$3H_2O + 2Mn(VII) \longrightarrow O_3 + 2Mn(IV)$$

$$O_3 + Mn(IV) \longrightarrow O_2 + \cdot O \cdot$$

$$O_3 + H_2O + Mn(IV) \longrightarrow O_2 + 2HO \cdot$$

$$Graphite + O_3 + 2HO \cdot + \cdot O \cdot \longrightarrow Graphene\ Oxide$$
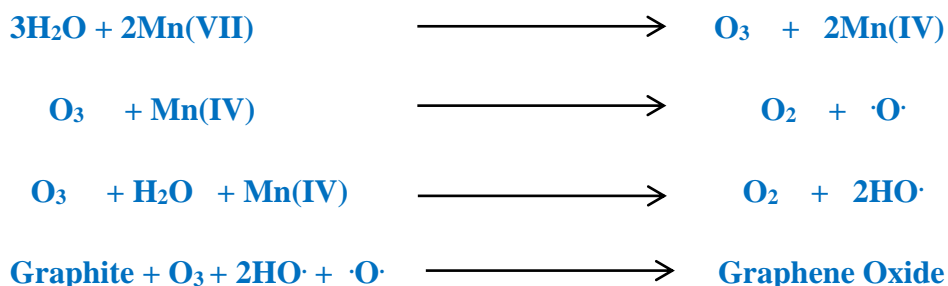
The solution then placed in an ice bath for controlling the sudden elevation in temperature. After 1 hour added 375mL of deionized water and placed it in the water bath at 90°C the suspension becomes thick due to heating then added 2mL of hydrogen peroxide (**H$_2$O$_2$**). Hydrogen peroxide removed the remnants of potassium permanganate. After the addition of hydrogen peroxide, centrifuged the mixture at 6000 rpm and washed with deionized water.

Add 1 mL of 1M solution of HCl and repeatedly add deionized water to remove permanganate and manganese dioxide salts. Again centrifuged mixture and washed with deionized water at 6000 rpm for 30mins. This layer by layer washing is known as chemical exfoliation. Take the mixture and placed it a hot plate with stirring for 1 hour. Now precipitates were dried at 60-70°C in the oven and obtained dried precipitate is Graphene Oxide (GO).

Synthesis of Graphene Oxide (GO)

1

Take 75mL H_2SO_4 in 250 mL Beaker

Constant stirring (1h) → ← 4g expanded graphite

Put the beaker on ice bath

Stirring and add 375mL D/H_2O → ← Add 12g $KMnO_4$ in 3 intervals

Use water bath → ← Heating for 2 hours(90°C)

Add 2 mL of H_2O_2

2

300mL Distilled water

← Stirring for 1hour

7 mL of 1M HCL Solution → ← Add 250 mL DI water

Centrifugation (6000 rpm) for 15-30 minute

Stirring for 1 h → ← Add 250 mL DI water

Centrifugation (6000 rpm) for 15-30 minute

Dry the paste on Hot plate at 60-70 °C

The dry mass is Graphene Oxide

Fig 3.2 Schematic depiction of synthesis of expanded graphite

3.2.2 Synthesis of aromatic diamines azo dyes

Five novel azo-dyes were synthesized based on coupling reaction involving two basic steps

- Synthesis of diazonium ion from an aniline derivative.

- Coupling of diazonium ion with an aromatic compound.
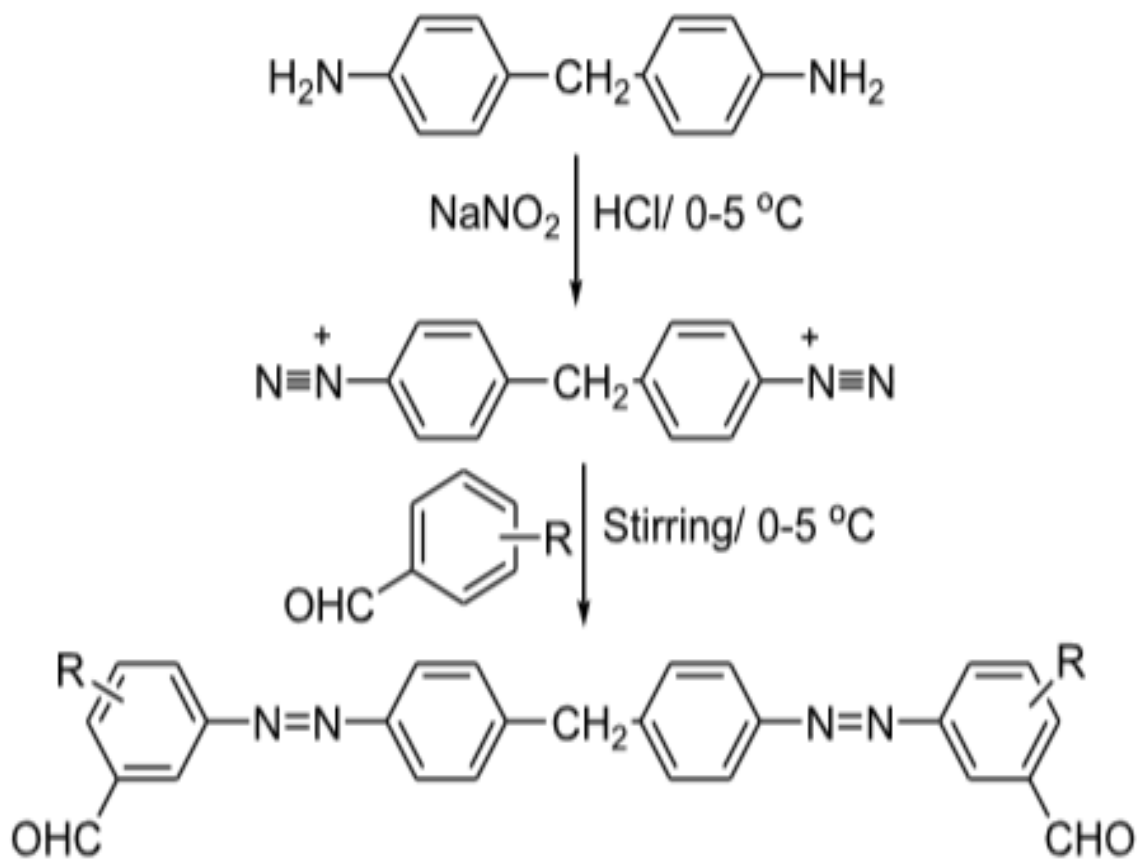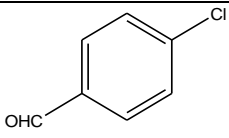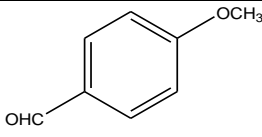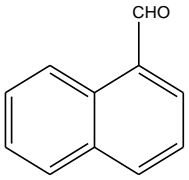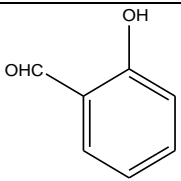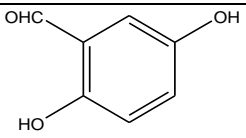
Fig 3.3 Schematic depiction for the synthesis of azo dyes

Five novel azo dyes have different couplers to form a couple with aniline derivatives. The coupler names and structure of five azo dyes are as shown in the Table 3.2.

Table 3.2 Coupler names and structures

IUPAC Names	Abbreviation Names	Structure
4-Cholorobenzaldehyde	HT (1-1) Coupler	
4-methoxy benzaldehyde	HT (1-2) Coupler	
1-naphthaldehyde	HT (1-3) Coupler	
2-hydroxybenzaldehyde	HT (1-4) Coupler	
2,5-dihydroxybenzaldehyde	HT (1-5) Coupler	

3.3 Characterization of Materials and Samples

The samples were characterized by using the following techniques

3.3.1 Fourier Transform Infra-Red Spectroscopy (FT-IR)

FT-IR analysis of the prepared samples was carried out on Thermo Scientific Nicolet iS10. The analysis was carried out at a range of 4000-600cm^{-1}wave numbers. FTIR was done for the recognition of different functional groups in an organic compound. It is a sensitive technique and can also differentiate some inorganic compounds such as paints, resins, polymers, drugs, and coatings. It is a very useful technique used to isolate and characterize organic contamination[81].

3.3.2 UV-Visible Spectrophotometer

The analysis was done on the spectrophotometer of Model UV-1800, Pharmaspec Shimadzu, Japan. The substances having π-electrons or non-bonding electrons have the tendency to absorb energy in the form of ultra-violet or visible light to excite pi-electrons to higher energy orbits. The energy necessary for different transitions follow the following order σ-σ*>n-σ*>π-π*>n-π*.

3.4 Procedure of Stock solution

500 ppm solution was prepared by using 1 mmol (millimole) dyes in 5mL of DMSO. Various ppm (parts per million) solutions were made from stock solution by taking a specific quantity of stock solution and making the volume up to 100 mL water. All solutions of 5 ppm were prepared for the study of parameters required for the spectroscopic process.

3.5 Spectroscopic measurements

UV-Vis spectrophotometer gives absorbance values of molecules after the excitation of electrons. Absorbance values of azo dyes observed before and after adsorption. Further compared their absorbance values with molar absorptivity and found concentrations of each solution. It describes a linear relationship between concentrations and absorbance of absorbing the class of compounds.

3.6 Batch sorption techniques

These studies were used to conduct adsorption along with factors affecting adsorptions *i.e.,* adsorbent dose, contact time, which impact the rate of dye adsorption by Graphene Oxide nanoparticles. Five novel azo-dyes (HT 1-1), (HT 1-2), (HT 1-3), (HT 1-3), (HT 1-4), and (HT 1-5) solutions of numerous concentration were arranged in volumetric flasks. Nanoparticles (as adsorbent) were added in each flask and the flasks were put in a shaker until the equilibrium between dye and adsorbent was maintained. The solution of each flask was filtered and absorbance of liquid was measured by UV-Vis spectrophotometer[82]. The number of azo-dyes adsorbed on Graphene Oxide nanosheet was obtained by the equation as follows:

$$Adsorption\ Capacity(q_e) = \frac{C_i - Ce}{C_i} \times \frac{V}{M} \qquad \qquad 3.1$$

C_i = *initial dye concentration*

C_e = *equilibrium dye concentration*

V = *volume of dye solution*

M = *mass of nanoparticles*

Dye amount adsorbed by absorption from UV-Vis spectroscopy calculated by formula as follows:

Amount Adsorbed (nm) = Initial Absorbance – Final Absorbance   3.2

3.7 Factors Affecting the Rate of Adsorption of Dyes onto Nanoparticles

3.7.1 Graphene Oxide Dosage Effect

Six standard solutions of 5 ppm concentration were prepared from each azo-dyes stock solution. Optimum pH was maintained of all the solutions. Different quantity of adsorbent varying from 0.01, 0.03, 0.05, 0.07, 0.09 and 0.1g was added in each flask. The solutions were shaken at optimum shaking speed and at a fixed time. Then the solutions were filtered and their absorbance was measured by spectrophotometer for the calculation of the best quantity of adsorbent for contact time study.

3.7.2 Interaction study of adsorption from Contact Time

Make three different concentrations of five novel azo-dyes (HT 1-1), (HT 1-2), (HT 1-3), (HT 1-4), and (HT 1-5) from stock solution at 298K temperature. Graphene oxide 0.05 gram was obtained as the best quantity for adsorption of dyes from the effect of dosage so this fixed amount of adsorbent (GO nanoparticles) was added in each of the solutions. The measuring flasks were shaken at 50 RPM on agitator within the time limit changing from 10 to 45 minutes. Then the solutions were filtered and their absorbance was measured for the calculation of adsorption capacity and dye removal percentage.

3.7.3 Adsorption Isotherms

Two adsorption isotherms studied were Langmuir and Freundlich isotherms. Comparing both graphs by finding the linear regression factor R^2 (0 to 1). Indicate bonds on the value of ΔG nature of adsorption *i.e.,* chemisorption and physisorption were determined.

$$\Delta G = -RT \, ln \, K_{ad} \qquad\qquad 3.3$$

$$\Delta G = \Delta H - T \, \Delta S \qquad\qquad 3.4$$

where K_{ad} = adsorption constant, T = absolute temperature in kelvin, and R = real gas constant with a value of 8.314 $Jmol^{-1}K^{-1}$.

1. If ΔG<0, the process occurs spontaneously.
2. If ΔG=0, the system is at equilibrium.
3. If ΔG>0, the process occurs spontaneously in the opposite direction[83].

The current work is focused to explore the adsorption behavior of five azo-dyes on Graphene Oxide using density functional theory (DFT). According to Quantum Mechanics, all the possible information regarding the electronic structure and the corresponding properties of a molecule can be derived directly from wave function which is obtained by solving the time-independent Schrödinger Wave equation for a multinuclear and multi-electron system[84].

$$H \Psi = E \Psi \qquad\qquad 3.5$$

Ψ is a many-electron wave function, E is the Eigenvalue of the operator (total energy of the system) and H is the called Hamiltonian operator.

3.8 Computational Modeling suite

Presently SCM Amsterdam Density Function Modeling suite 2019 has been employed as a powerful tool for heterogeneous adsorption of five novel azo dyes on the surface of Graphene Oxide (GO). Some important features of ADF.2017 modeling include

1. ADF is strong in understanding and predicting structure, reactivity, and spectra of molecules.

2. ADF offers unique aptitudes to calculate molecular properties of nanoparticles and organic electronics materials.
3. DFT calculations are easily prepared and analyzed with an integrated Graphical user interface (GUI).
4. ADF offers unique aptitudes to calculate molecular properties of nanoparticles and organic electronics materials.
5. ADF has modern Correlation (xc) functionals and all type of basis sets.

Amsterdam density function builder was used to create input structure files of azo-dyes and Graphene Oxide. In ADF density functional theory applied to study adsorption between azo-dyes and Graphene

Oxide at 3.5 Å distance. Firstly, input structures were created for all five dyes and Graphene Oxide in .xyz format. From geometric optimizations, determine HOMO-LUMO gaps, Adsorption energy (Ea), and Infrared spectrum. Frequency calculation provided entropy, enthalpy, heat capacity, Gibb's free energy, Hirshfield charge analysis, and adsorption constant.

The schematic presentation methodology used in computational software as shown below:
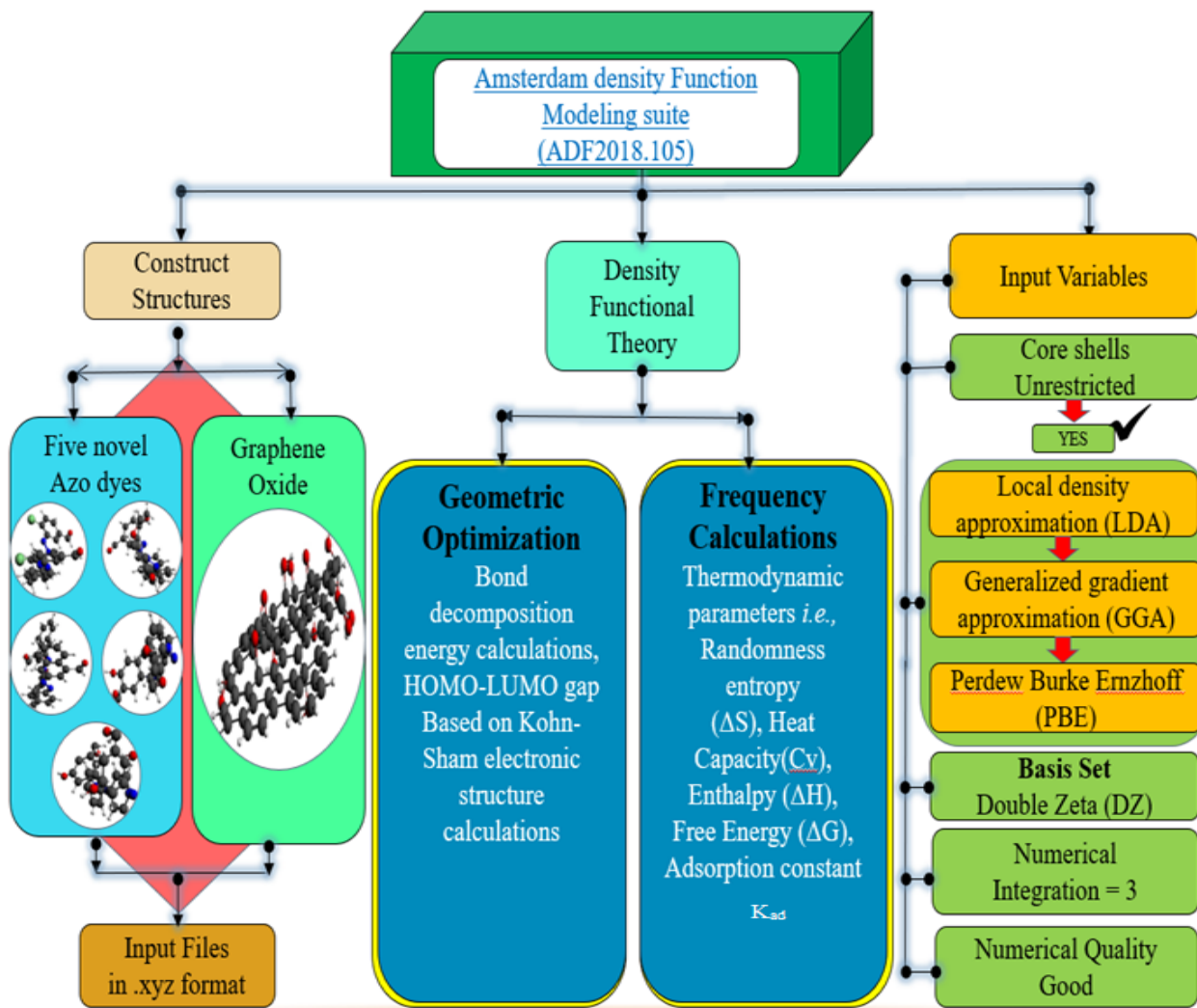
Fig 3.4 Methodology flow chart for computational modeling

Chapter 4

Results and Discussions

SECTION-I : EXPERIMENTAL RESULTS AND DISCUSSIONS

This section deals with experimental results and their interpretation for five novel azo-dyes on the surface of Graphene Oxide (GO) nanosheet. The experimental section included structural characterizations by means of FT-IR, and UV-Vis spectrophotometry and adsorption analysis including effect of dosage, contact time and Langmuir adsorption isotherm at 298 Kelvin temperature.

4.1 Characterizations of Graphene Oxide (GO)

4.1.1 FT-IR Spectroscopy of Graphene Oxide (GO)

The spectral analysis helps to recognize the presence of reactive functional groups in the structure of GO. Fig 4.1 shows the FT-IR spectrum peaks of Graphene Oxide (GO).
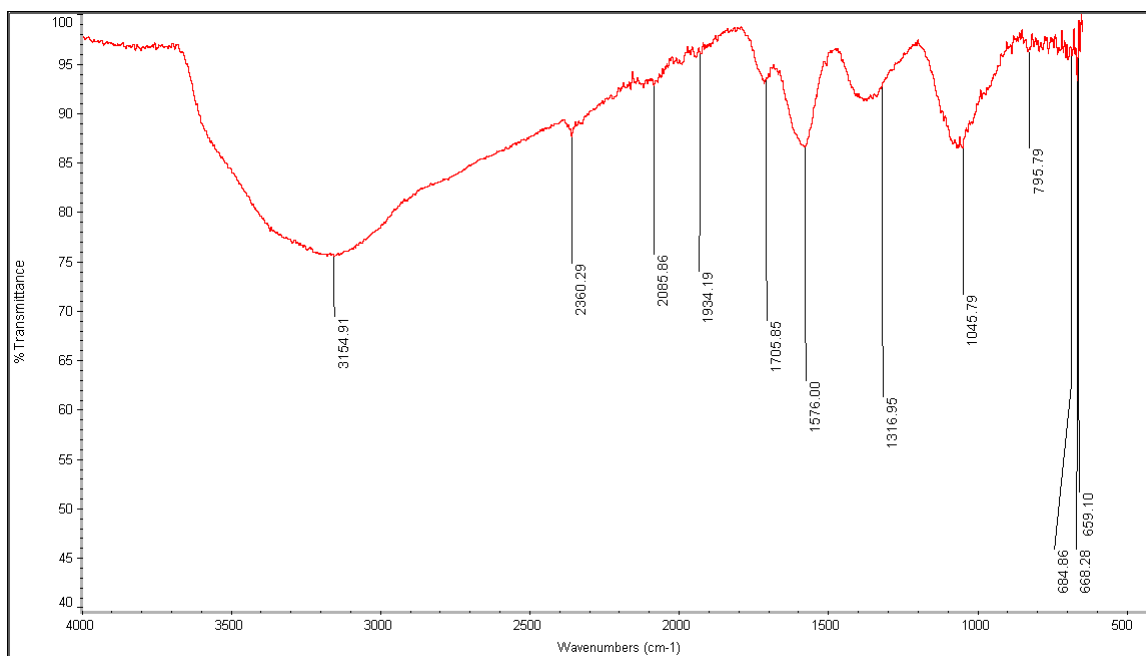
Fig 4.1 FT-IR spectrum of Graphene Oxide (GO) at 298 K temperature

A strong and broad peak was observed at about 3154.19 cm^{-1}, indicating the stretching vibration of an O-H group, confirming the presence of hydroxyl groups in obtained GO. The intense peaks at 1705.85 cm^{-1} recognized to the formation of C=O groups in Graphene Oxide, while the peaks at 1576.00 cm^{-1} and 1045.79 cm^{-1} indicated the presence of carbon-carbon double bond and C-O (epoxy) groups.

4.1.2 UV-Visible Spectroscopy of Graphene Oxide (GO)

The UV-visible spectroscopic analysis helps to classify the existence of conjugation in a molecule. Fig 4.2 shows the UV-Visible spectrum peaks of Graphene Oxide (GO).
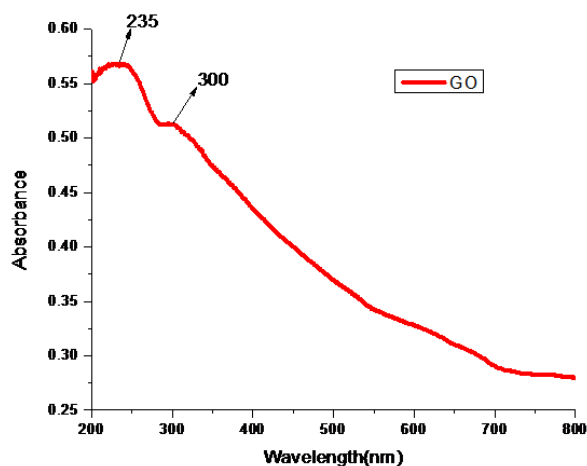
Fig 4.2 UV-Vis spectrum of Graphene Oxide at 298 K temperature

The maximum absorbance of Graphene Oxide (GO) was observed at 235 nm as depicted in Fig 4.2. This absorbance attributed to the electronic transition in C=C of aromatic groups. This transition is because of the conjugated π-electron system. The other shoulder peak which was observed at 300 nm showed the presence of carbonyl groups (C=O).

4.2 Factors Affecting the Rate of Adsorption

4.2.1 Effect of Graphene Oxide dosage

It was observed that 5ppm concentration of all adsorbate (azo-dyes) namely, Bis-3,3'-(4,4'-Diazenyldiphenylmethane)-4-chlorobenzaldehyde,Bis-3,3'-(4,4'-Diazenyldiphenylmethane)-p-anisaldehyde,Bis-3,3'-(4,4'-Diazenyldiphenylmethane)-naphthaldehyde,Bis-3,3'-(4,4'-Diazenyldiphenylmethane)-salicylaldehyde, and Bis-3,3'-(4,4'-Diazenyldiphenylmethane)-2,4-dihydroxybenzaldehyde were decreased after adding various quantities of the adsorbent dosage. Increasing amount of adsorbent (GO) resulted in greater decrease of adsorbate absorbance with no peak shift. No peak shift in absorbance is indicative of physisorption of azo-dyes on the surface of GO. values, Fig 4.3 (A-E) showed a graphical plot of best interacting dosage amount of adsorbent *i.e.,* 0.05g with all azo-dye adsorbate HT (1-1), HT (1-2), HT (1-3), HT (1-4), and HT (1-5). Fig 4.4 (A-E) revealed that UV-Vis absorption for all azo-dyes HT (1-1), HT (1-2), HT (1-3), HT (1-4), and HT (1-5) was decreased interacting with Graphene oxide (GO) at its different concentration due to formation of azo dye-GO complexes.

Table 4.1 Effect of Graphene oxide dosage on the absorbance of fixed concentration of azo-dyes (HT 1-1), (HT 1-2), (HT 1-3), (HT 1-4), and (HT 1-5) at 298K using UV-Vis spectrophotometer

Adsorbent Dosage (g)	(HT 1-1) Absorbance (nm)			(HT 1-2) Absorbance (nm)			(HT 1-3) Absorbance (nm)			(HT 1-4) Absorbance (nm)			(HT 1-5) Absorbance (nm)		
	Initial	After	Total	Initial	After	Total	Initial	After	Total	Initial	After	Total	Initial	After	Total
0.01	0.551	0.504	0.047	0.164	0.16	0.004	0.20	0.198	0.002	0.203	0.194	0.009	0.225	0.206	0.019
0.03	0.551	0.501	0.05	---	---	---	---	---	---	0.203	0.192	0.011	0.225	0.192	0.033
0.05	0.551	0.43	0.121	0.164	0.139	0.025	0.20	0.184	0.016	0.203	0.164	0.039	0.225	0.171	0.054
0.07	0.551	0.423	0.128	0.164	0.133	0.027	---	---	---	---	---	---	0.225	0.16	0.064
0.09	0.551	0.399	0.152	0.164	0.131	0.033	0.20	0.179	0.021	0.203	0.159	0.044	0.225	0.146	0.079
0.1	0.551	0.383	0.168	0.164	0.127	0.037	0.20	0.177	0.023	0.203	0.155	0.048	---	---	---
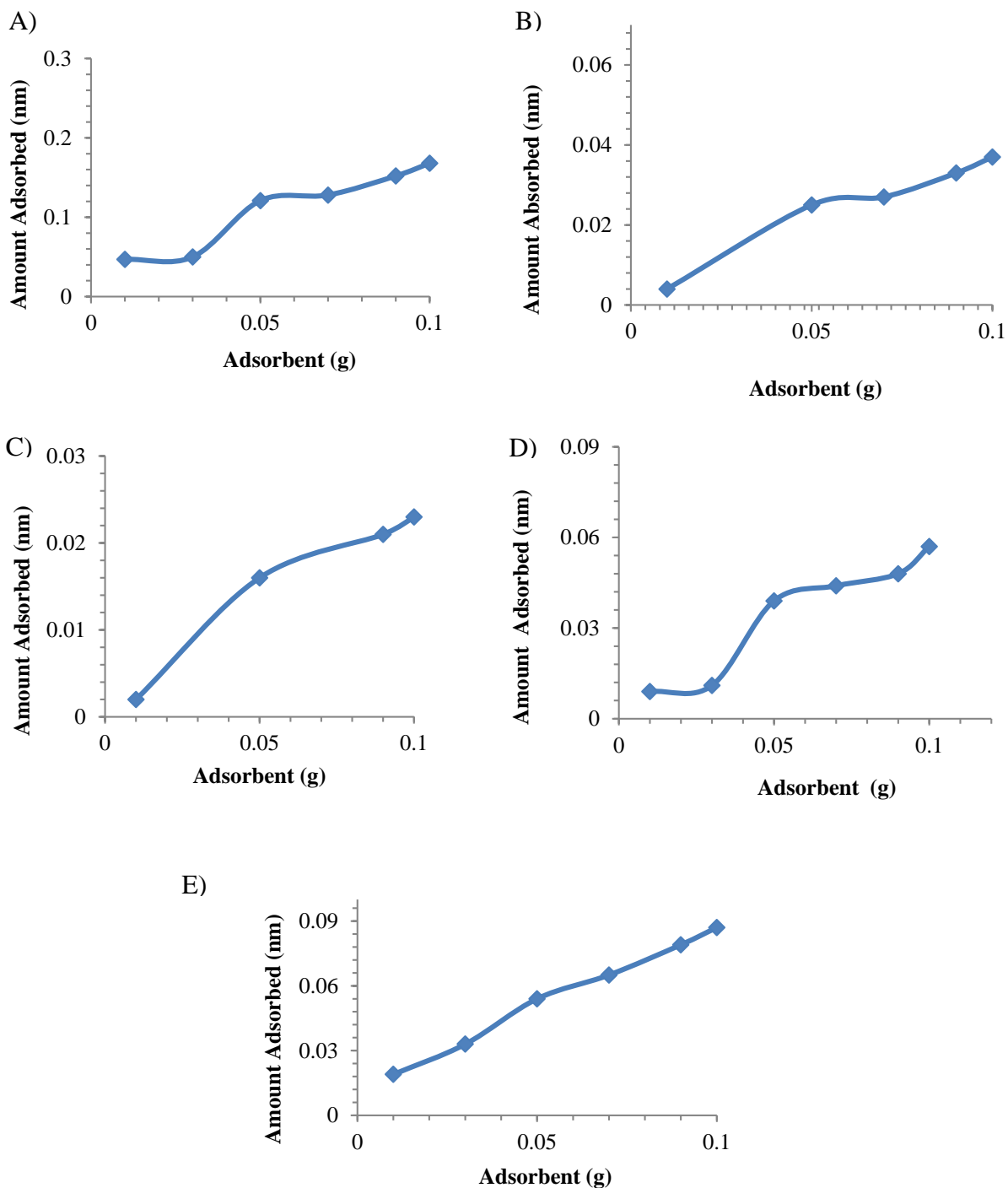
Fig 4.3 Graphical representation of the effect of dosage on Graphene Oxide at a fixed concentration of azo-dyes A) (HT 1-1), B) (HT 1-2), C) (HT 1-3), D) (HT 1-4), and E) (HT 1-5) at 298K temperature using UV-Vis spectroscopy
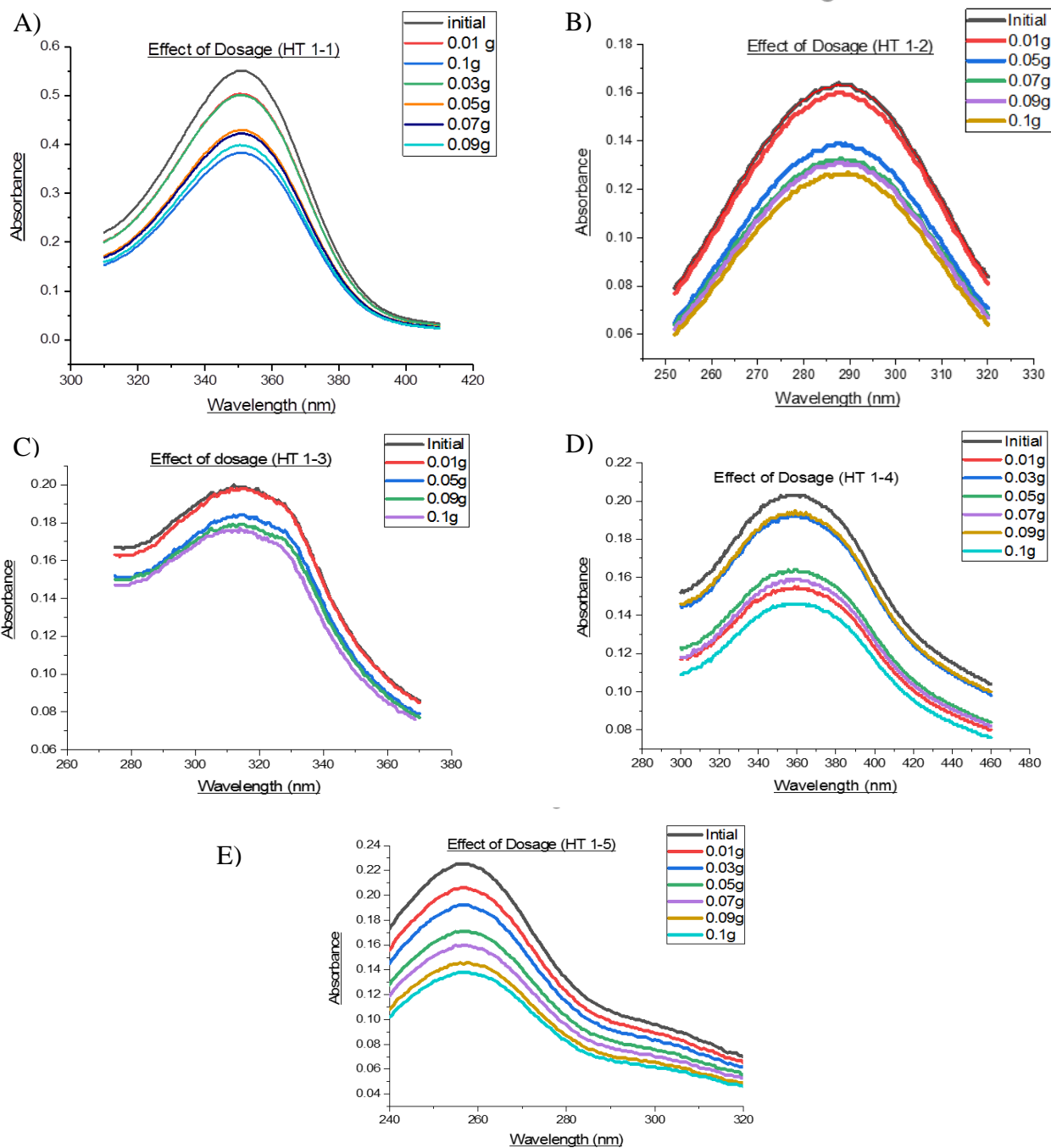
Fig 4.4 UV-Vis Spectral representation of the effect of Graphene Oxide dosage at a fixed concentration of azo-dyes A) (HT 1-1), B) (HT 1-2), C) (HT 1-3), D) (HT 1-4), and E) (HT 1-5) at 298K temperature

4.2.2 Effect of Contact Time

Contact time studied was analyzed by means of 0.05g dosage of adsorbent (GO) and observed decrease in concentrations of all adsorbate (azo-dyes) namely, Bis-3,3'-(4,4'-Diazenyldiphenylmethane)-4-chlorobenzaldehyde,Bis-3,3'-(4,4'-Diazenyldiphenylmethane)-p-anisaldehyde,Bis-3,3'-(4,4'-Diazenyldiphenylmethane)-naphthaldehyde,Bis-3,3'-(4,4'-Diazenyldiphenylmethane)-salicylaldehyde, and Bis-3,3'-(4,4'-Diazenyldiphenylmethane)-2,4-dihydroxybenzaldehydeat different time intervals starting from 0 – 45 min. Different concentrations of dyes were selected based on their interaction with fixed conc. of GO. Fig 4.5 (A-E) showed that maximum interaction between azo dyes and Graphene oxide (GO) took place at 20 min, after 20 min time absorbance tends to consistent indicating that equilibrium between interaction of azo dyes and Graphene oxide (GO) has taken place. Absorbance remains consistent even till 45 min. A graphical plot of decrease in three various concentrations of azo-dyes HT (1-1), HT (1-2), HT (1-3), HT (1-4), and HT (1-5) with fixed amount of adsorbent *i.e.,* 0.05g and maximum adsorption was observed at 20min for all azo-dyes after that it developed an equilibrium. This revealed that maximum interaction for complex formation between azo dyes and GO took place at 20 min.
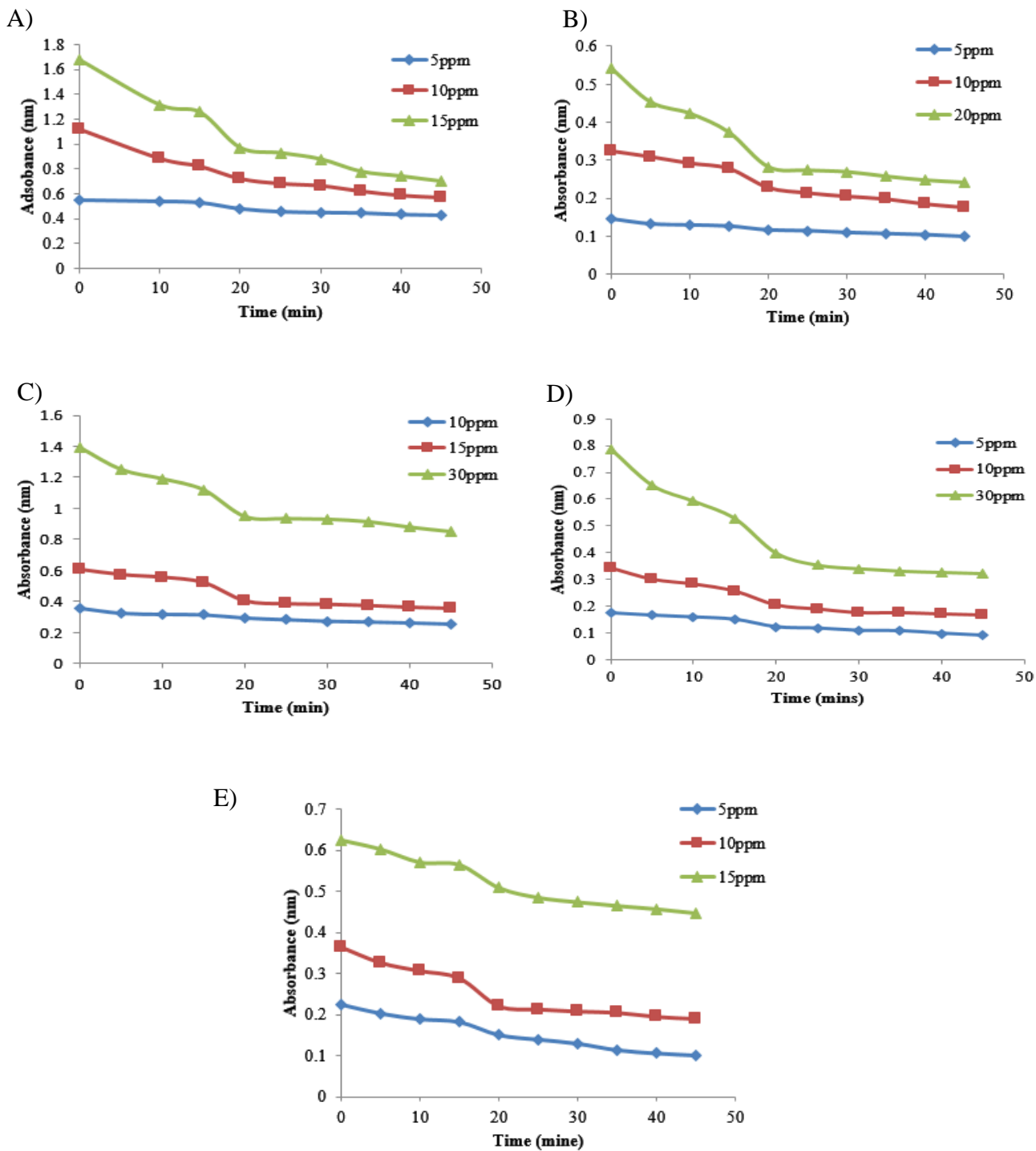
Fig 4.5 Graphical representation of Contact time study using 0.05g quantity of Graphene Oxide at some various concentrations of azo-dyes A) (HT 1-1), B) (HT 1-2), C) (HT 1-3), D) (HT 1-4), and E) (HT 1-5) at 298K temperature by means of UV-Vis spectroscopy

4.2.3 Adsorption Isotherms

Adsorption isotherms are the curves that show surface properties, adsorption affinity of adsorbents towards various contaminants and the equilibrium data confirms the adsorption behavior of solid molecules on adsorbent along with the mechanism of adsorption. Many of the adsorption models like Freundlich, Langmuir, Temkin, Koble Corrigan, and Dubinin Radushkevich were developed for adsorption study however, the most familiar and widely used adsorption isotherms are Langmuir and Freundlich.

4.2.3.1 Langmuir Isotherm

Langmuir adsorption model depends on thermodynamic parameters and this model states that there is a fixed number of sites over adsorbent surface forming homogeneous surface and every single site takes one atom, the adsorbed atom has no interaction with a bulk solution. The adsorbate molecules do not migrate due to the formation of adsorbate monolayer on the adsorbent surface and this is the driving force that provides maximum energy for adsorption[85].

The equation of Langmuir Isotherm is given below:

$$\frac{C_e}{q_e} = \frac{1}{K_L q_m} + \frac{C_e}{q_m} \qquad\qquad 4.1$$

where K_L : Langmuir adsorption constant, q_m : maximum adsorption capacity; q_e : adsorption capacity at equilibrium; C_e is concentration at equilibrium.

Comparing equation 4.1 and equation 1.1, calculated molar absorptivity (ε), concentrations, Langmuir adsorption constant (K_L), and q_m as shown in Table 4.2, Fig 4.6 and Fig 4.7.

Molar absorptivity(ε) was calculated from the slope of Fig. 4.6 followed by determination of equilibrium concentrations.

Langmuir adsorption isotherm (K_L) was calculated from the slope of Fig 4.7 followed by determination of adsorption free energy (ΔG) (Table 4.3).
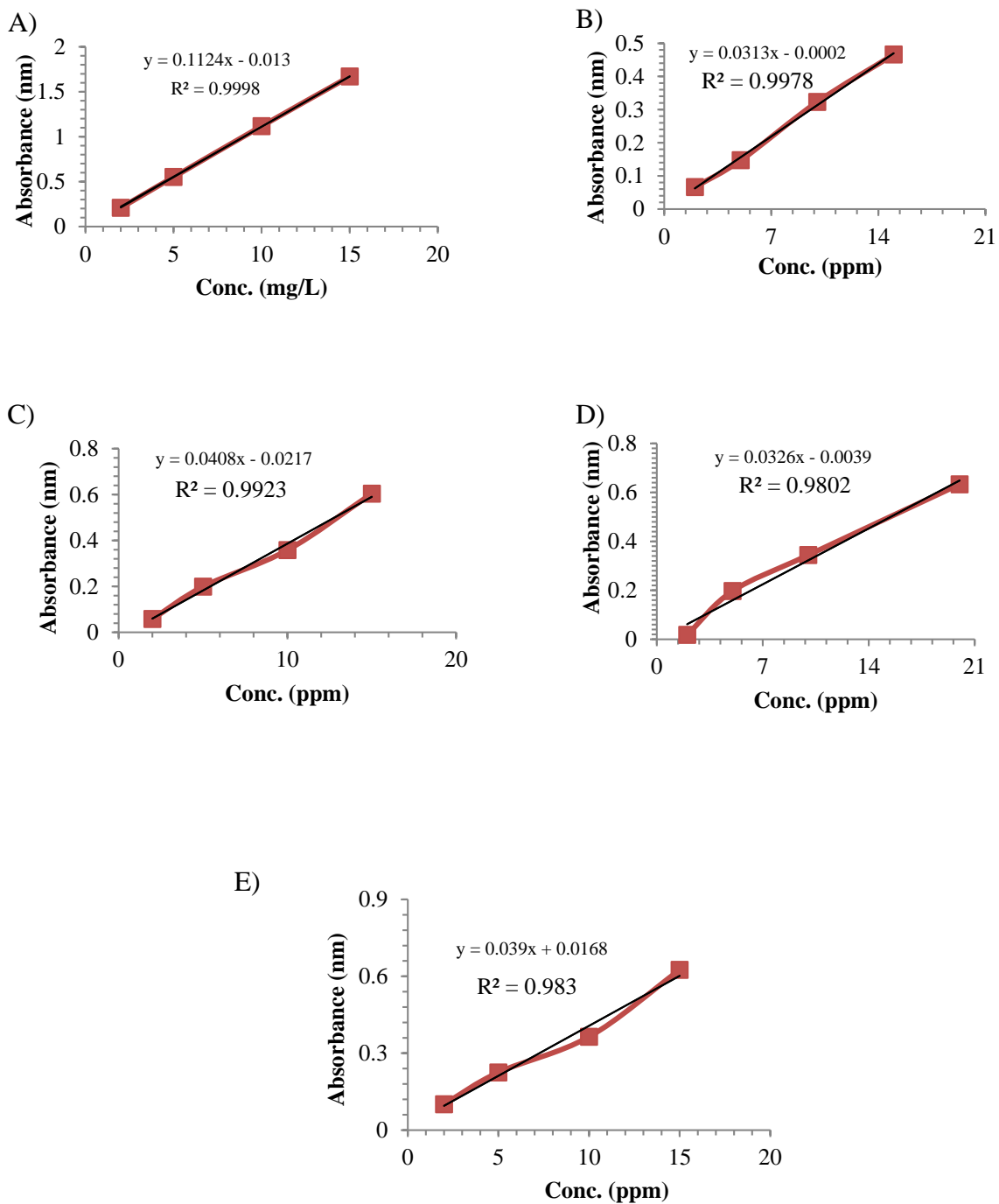
Fig 4.6 Graphical representation of various initial concentrations of azo-dyes A) (HT 1-1) $\varepsilon = 0.1124$, B) (HT 1-2) $\varepsilon = 0.0313$, C) (HT 1-3) $\varepsilon = 0.0408$, D) (HT 1-4) $\varepsilon = 0.0326$, and E) (HT 1-5) $\varepsilon = 0.039$ at 298K temperature by means of UV-Vis spectroscopy

Table 4.2 Tabulated data of Langmuir isotherm parameters to find Langmuir adsorption constant (K_L) at 298K

Conc. ppm	(HT 1-1)			(HT 1-2)			(HT 1-3)		
	Ce (ng/L)	qe (mg/g)	Ce/qe (µg/g)	Ce (ng/L)	qe(mg/g)	Ce/qe (µg/g)	Ce (ng/L)	qe(mg/g)	Ce/qe (µg/g)
2	1.27×10^{-9}	0.728	1.75×10^{-6}	1.41×10^{-9}	0.594	1.11×10^{-6}	1.05×10^{-9}	0.946	1.11×10^{-6}
5	---	---	---	3.71×10^{-9}	0.518	1.29×10^{-5}	4.10×10^{-9}	0.360	1.14×10^{-5}
5.7	---	---	---	---	---	---	---	---	---
6	3.83×10^{-9}	0.723	5.31×10^{-6}	---	---	---	---	---	---
10	6.40×10^{-9}	0.721	8.88×10^{-6}	7.25×10^{-9}	0.550	1.45×10^{-5}	7.21×10^{-9}	0.558	1.29×10^{-5}
15	8.62×10^{-9}	0.851	1.01×10^{-5}	9.25×10^{-9}	0.730	1.30×10^{-5}	9.88×10^{-9}	0.683	1.45×10^{-5}

Conc. ppm	(HT 1-4)			(HT 1-5)		
	Ce (ng/L)	qe (mg/g)	Ce/qe (µg/g)	Ce (ng/L)	qe (mg/g)	Ce/qe (µg/g)
2	3.99×10^{-10}	1.601	2.49×10^{-7}	---	---	---
2.5	---	---	---	1.72×10^{-9}	0.282	6.09×10^{-6}
5.7	---	---	---	3.85×10^{-9}	0.461	8.33×10^{-6}
6	4.57×10^{-9}	0.476	9.59×10^{-6}	---	---	---
7	---	---	---	6.25×10^{-9}	0.214	7.67×10^{-6}
9	---	---	---	1.31×10^{-8}	0.259	5.02×10^{-5}
10	1.65×10^{-8}	0.754	8.25×10^{-6}	---	---	---
20	4.12×10^{-8}	0.653	2.06×10^{-5}	---	---	---

A)

y = 1169.2x + 6E-07

R² = 0.9734

B)

y = 1378.1x + 1E-06

R² = 0.9156

C)

y = 1421x + 2E-06

R² = 0.8074

D)

y = 1506.6x + 4E-07

R² = 0.9611

E)

y = 1240.5x + 8E-07

R² = 0.9832
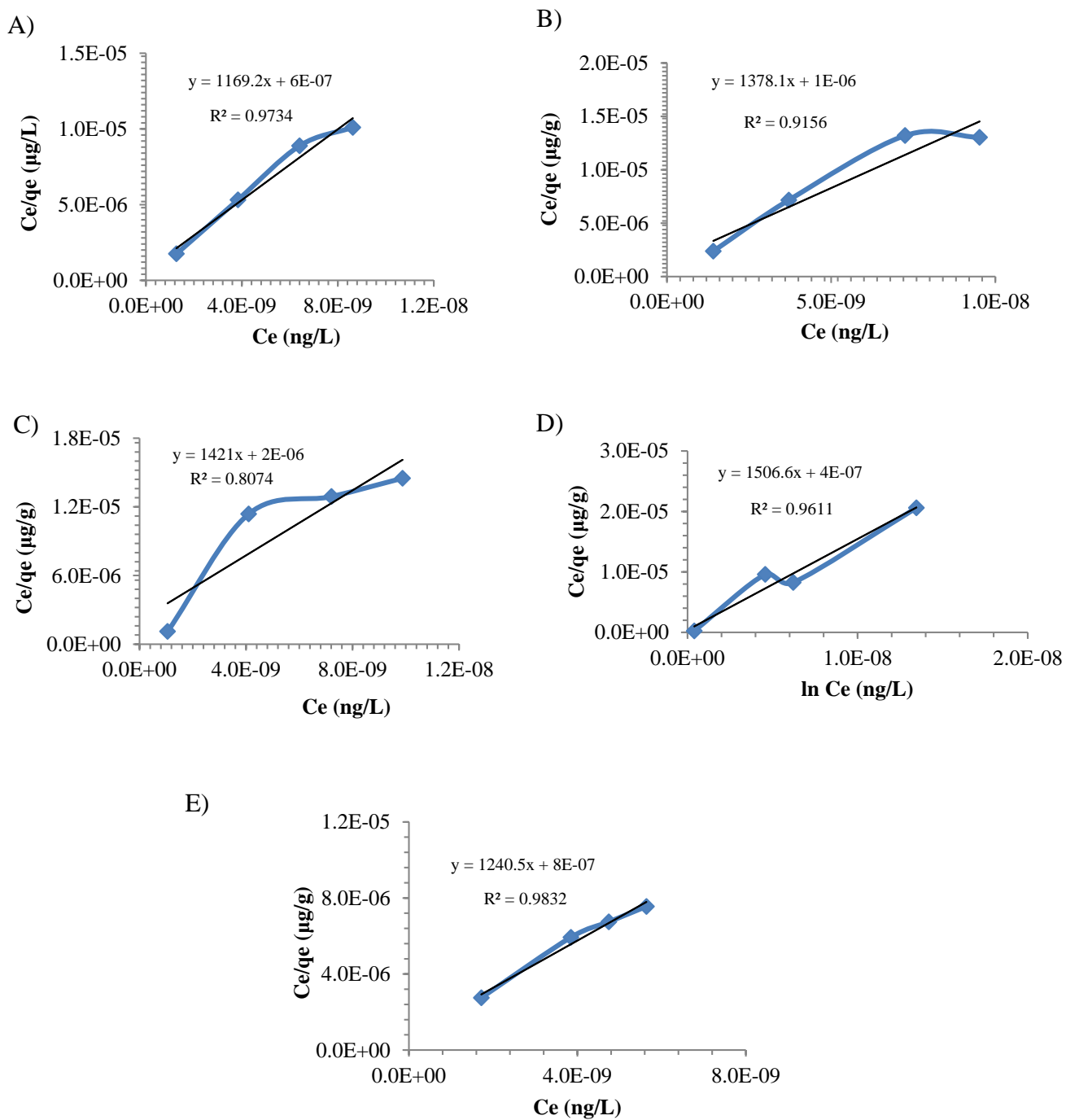
Fig 4.7 Graphical representation of Langmuir adsorption isotherm of adsorbed azo-dyes A) (HT 1-1), B) (HT 1-2), C) (HT 1-3), D) (HT 1-4), and E) (HT 1-5) on GO at 298K temperature using of UV-Vis spectroscopy

4.2.4 Experimental data interpolation

Experimental data revealed that adsorption constant (K_{ad}) values of azo dye (HT 1-4) was higher as compared with other azo dyes (HT 1-1), (HT 1-2), (HT 1-3), and (HT 1-5) because of its strong intermolecular interaction of -OH and -CHO group of (HT 1-4) coupler with graphene oxide -COC group, hence it has the highest affinity of adsorption on the surface of Graphene Oxide. Free energy also revealed that azo dye (HT 1-4) interactions are more spontaneous as compared to other dyes as shown in Table 4.3.

Azo dyes (HT 1-3) adsorption constant value was less as compared to other azo dyes (HT 1-1), (HT 1-2), (HT 1-4), and (HT 1-5) due to its conjugation and pi - pi intramolecular interactions between aromatic rings of (HT 1-3) coupler *i.e.,* 1-naphthaldehyde and carbon hexagone of Graphene oxide (GO), hence have less interaction with graphene oxide nanoparticle as shown in Fig 4.8.
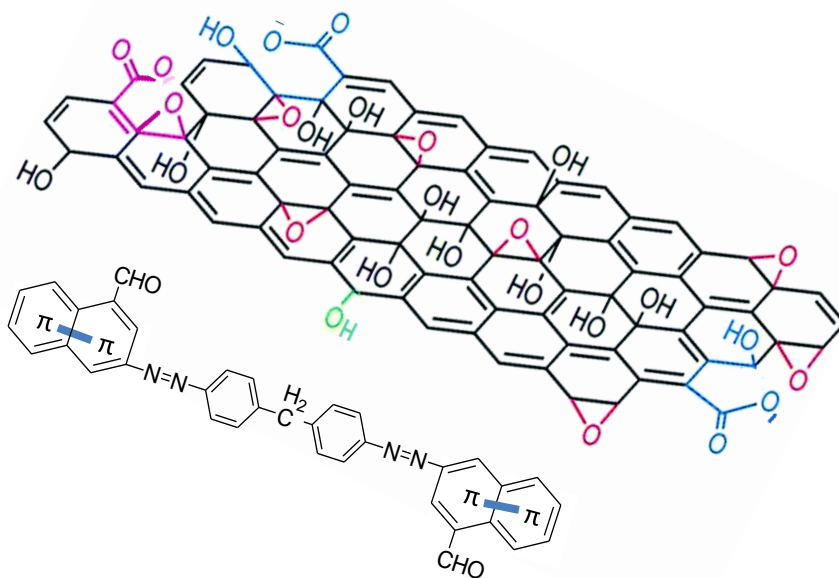
Fig 4.8 Scheme of azo-dye (HT 1-3) adsorption on Graphene Oxide (GO) at 298K

All azo-dyes (HT 1-1), (HT 1-2), (HT 1-3), (HT 1-4), and (HT 1-5) adsorbed on the surface graphene oxide nanoparticle by means of weak Van der Waals forces of interaction which revealed physisorption reaction.

Table 4.3 Thermodynamic parameter calculations from experimental adsorption of azo dyes (HT 1-1), (HT 1-2), (HT 1-3), (HT 1-4), and (HT 1-5) at 298K temperature.

S.NO	Langmuir adsorption constant Temp = 298 K		Gibbs Free Energy $\Delta G = -RT \ln(K_L)$
Composite	R^2	K_L	J/mol
(HT 1-1)+GO	0.9734	1.948×10^9	-5299.5
(HT 1-2)+GO	0.9156	1.378×10^9	-5213.7
(HT 1-3)+GO	0.8074	7.105×10^8	-5049.6
(HT 1-4)+GO	0.9611	3.766×10^9	-5462.8
(HT 1-5)+GO	0.9832	1.550×10^9	-5243.9

Chapter 4

SECTION-II : COMPUTATIONAL RESULTS AND DISCUSSIONS

4.3 Electronic and Kinetic effect of Adsorption

Presently, five novel azo-dyes are studied for adsorption at 3.5 Å distance employing the computational DFT method. Electronic, kinetic and Thermodynamics, parameters were calculated to understand the energetic behaviors of compounds associated with physisorption and chemisorption. The general mechanism of reaction kinetic included adsorbent (A) interact with adsorbate (B) through a reversible or irreversible process. The reversible process can lead to physisorption whereas irreversible phenomena caused the chemisorption. General Mechanism for the adsorption of all azo dyes (adsorbate) with Graphene Oxide (adsorbent) can be presented as below :

$$K_f$$

$$A \text{ (adsorbent)} + B \text{ (adsorbate)} \quad \rightleftharpoons \quad A\text{-}B \text{ (physisorption)}$$

$$K_r$$
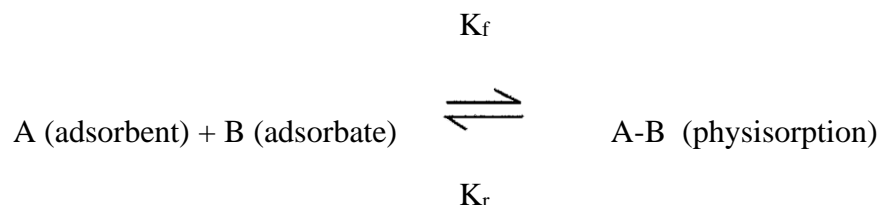
Herein, azo dyes exhibited chemisorption on the surface of Graphene Oxide (GO)

$$A \text{ (adsorbent)} + B \text{ (adsorbate)} \longrightarrow A\text{-}B \text{ (chemisorption)}$$
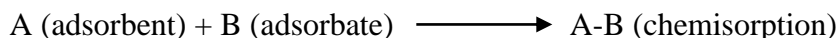
The energy of adsorption can be calculated using the following equation

$$\Delta E_{ads} = E_{(A\text{-}B)} - (E_A + E_B \ldots) \tag{4.2}$$

Whereas E_A is the energy of adsorbent A, E_B is the energy of the adsorbate B and $E_{(A\text{-}B)}$ is the energy of the complex[86]. In order to develop the better understanding of adsorption process, we have theoretically investigated parametric evaluation of enthalpy (ΔH), entropy (ΔS), adsorption constant (K_{ad}), frontier

molecular orbitals calculations (ELUMO and EHOMO) and Gibbs free energy (ΔG) after the adsorption of each azo dye determined the spontaneity of reaction and strength of complex between Graphene Oxide and azo-dyes. The result revealed that ΔE_{ads} for (HT 1-1) was positive value due to weakly deactivating -Cl group on aromatic ring of (HT 1-1) coupler while all others are negatively favored because they have strong deactivating group like –CHO, -OH and –OCH$_3$on their aromatic ring as shown in (Table 4.4).

Table 4.4 Energetic parameters for adsorption of azo dyes on the surface of Graphene Oxide (GO) calculated at LDA-GGA (Local density approximation–Generalized gradient approximation) level theory

S.NO	$\Delta E_{ads} = E_{Composite} - (E_{Dye} + E_{Graphene\ Oxide})$				Composite – (Dye + Graphene Oxide)
	Composite **Bond E kcal/mol**	Dyes **Bond E kcal/mol**	GO **Bond E kcal/mol**	Dyes + GO **Bond E kcal/mol**	ΔE_{ads} **kcal/mol**
(HT 1-1)	-25530.35	-7752.12	-17569.45	-25321.58	+208.77
(HT 1-2)	-21362.05	-8823.53	-17569.45	-26392.99	-5030.93
(HT 1-3)	-26941.68	-9772.58	-17569.45	-27342.03	-400.35
(HT 1-4)	-23479.33	-8017.94	-17569.45	-25587.39	-2108.05
(HT 1-5)	-22789.14	-8277.98	-17569.45	-25847.43	-3058.29

It was observed that azo dye (HT 1-3) has the highest value of adsorption energy ΔE_{ads} due to 1-naphthaldehyde (HT 1-3) coupler have high conjugation and arene - arene intramolecular interaction between aromatic rings while other azo–dyes couplers *i.e.,* 4-Cholorobenzenaldehyde (HT 1-1) coupler, 4-methoxybenzenaldehyde (HT 1-2) coupler, 4-hydroxybenzenaldehyde (HT 1-4) coupler, and 2,5-dihydroxybenzenaldehyde (HT 1-5) coupler have no such interactions.

4.3.1 Stability of adsorption based on E $_{HOMO}$ -E $_{LUMO}$ Gap

The ΔE (E $_{HOMO}$ -E $_{LUMO}$ Gap) played an essential role in the kinetic stability of the complex. The frontier orbitals effect dominated if smaller HOMO-LUMO gap is present between adsorbate and adsorbent and leads to greater overlap, hence have greater adsorption constant values. It was observed that the HOMO-LUMO gap of azo dyes (HT 1-1), (HT 1-2), (HT 1-4), and (HT 1-5) were significantly less indicating high electronic overlapping at distance 3.5 Å while azo dye (HT 1-3) has high electronic overlapping but its HOMO-LUMO gap was high *i.e.,* -7.95 kcal/mol compared to other azo dyes because of its stable 1-naphthoaldehyde coupler as shown in Fig 4.9 – 4.13 and (Table 4.5).

| E $_{LUMO}$ | -133.67 kcal/mol |

ΔE   0.77 kcal/mol

| E $_{HOMO}$ | -134.45 kcal/mol |
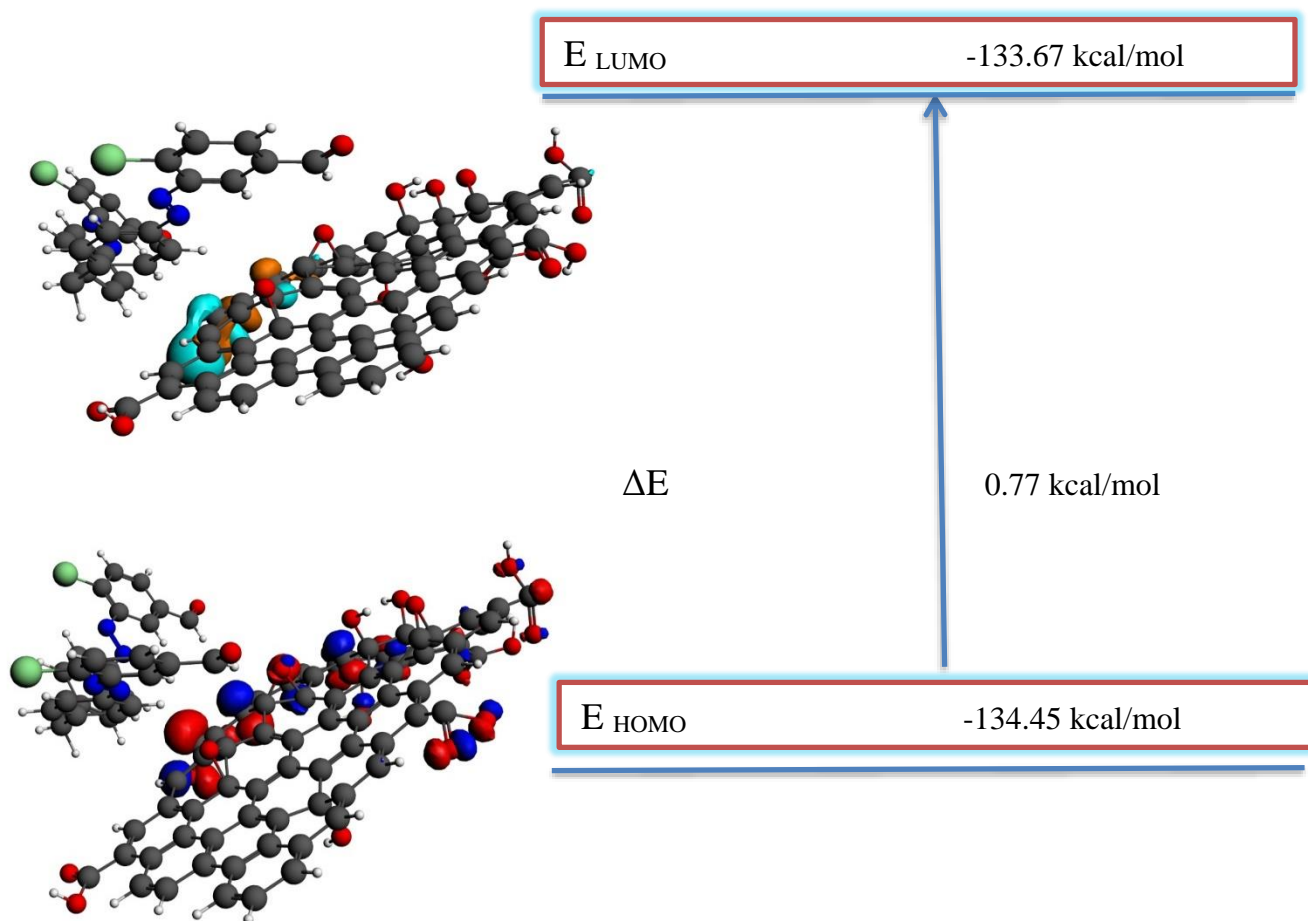
Fig 4.9: HOMO-LUMO gap of (HT 1-1) adsorbed on the surface of Graphene Oxide (GO)

E LUMO	-72.91 kcal/mol

ΔE   1.82 kcal/mol

E HOMO	-74.73 kcal/mol
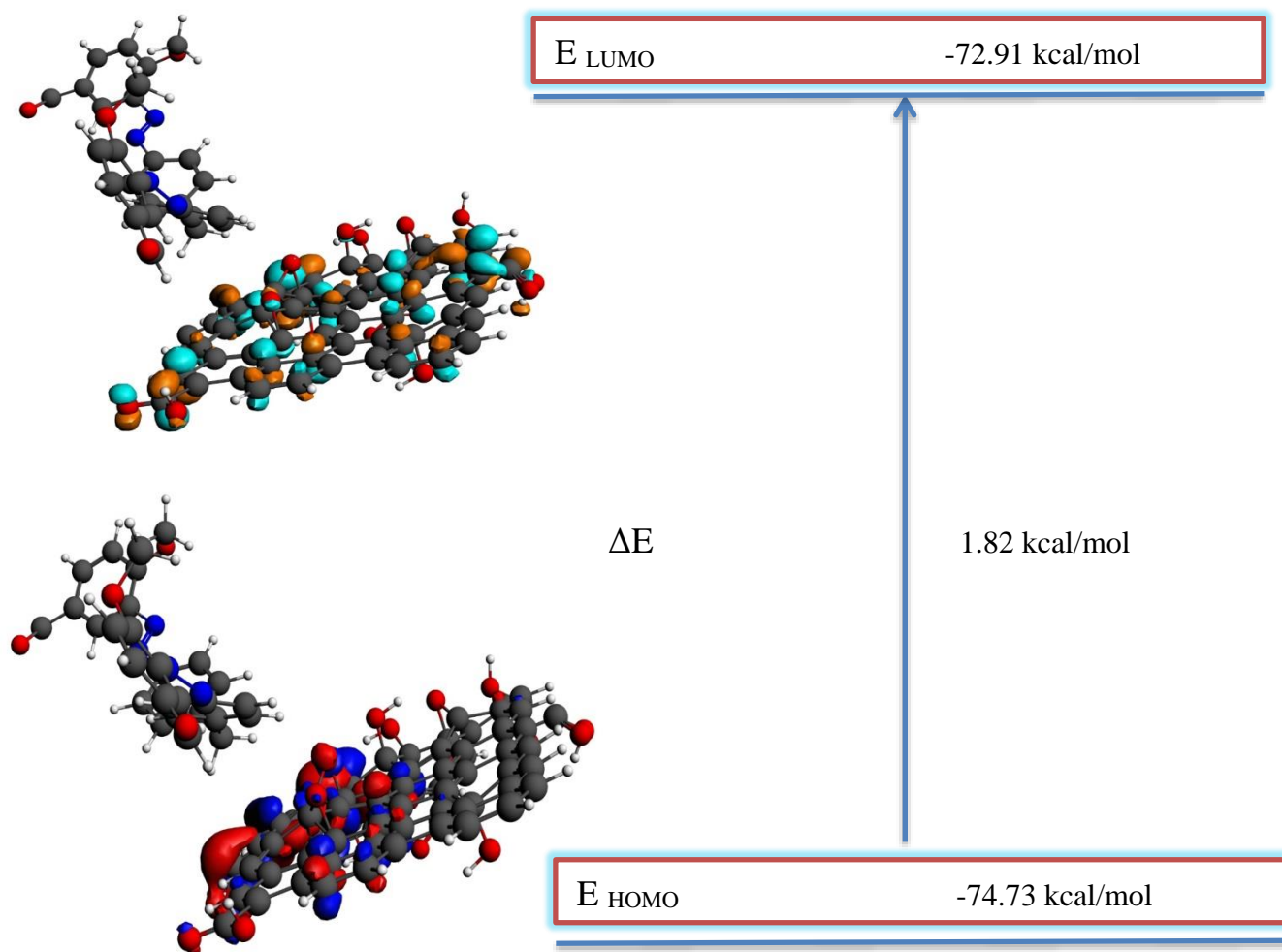
Fig 4.10: HOMO-LUMO gap of (HT 1-2) adsorbed on the surface of Graphene Oxide (GO)

| E LUMO | -103.65 kcal/mol |

ΔE   7.95 kcal/mol

| E HOMO | -111.61 kcal/mol |
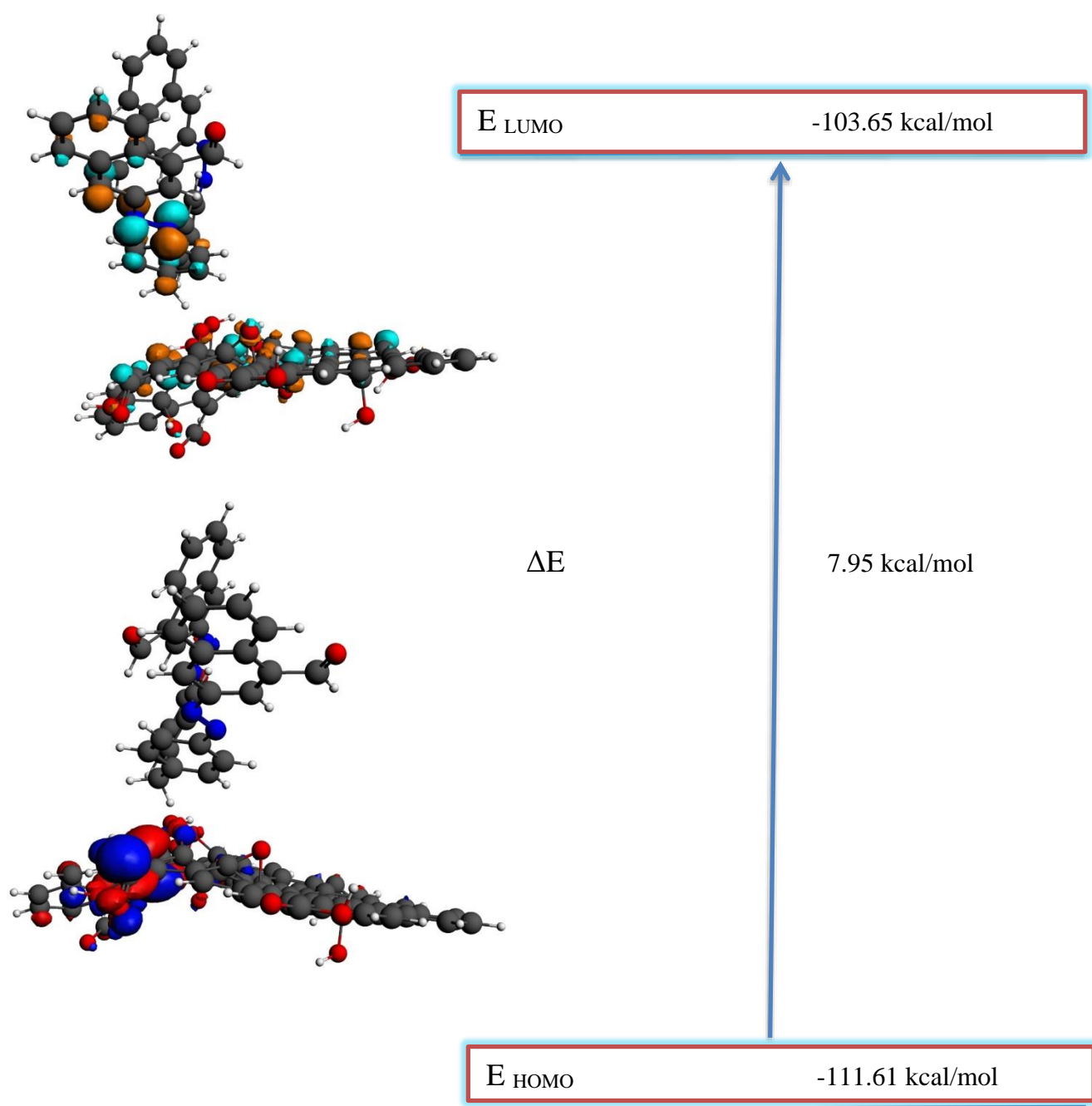
Fig 4.11: HOMO-LUMO gap of (HT 1-3) adsorbed on the surface of Graphene Oxide (GO)

| E LUMO | -51.96 kcal/mol |

ΔE   1.63 kcal/mol

| E HOMO | -53.59 kcal/mol |
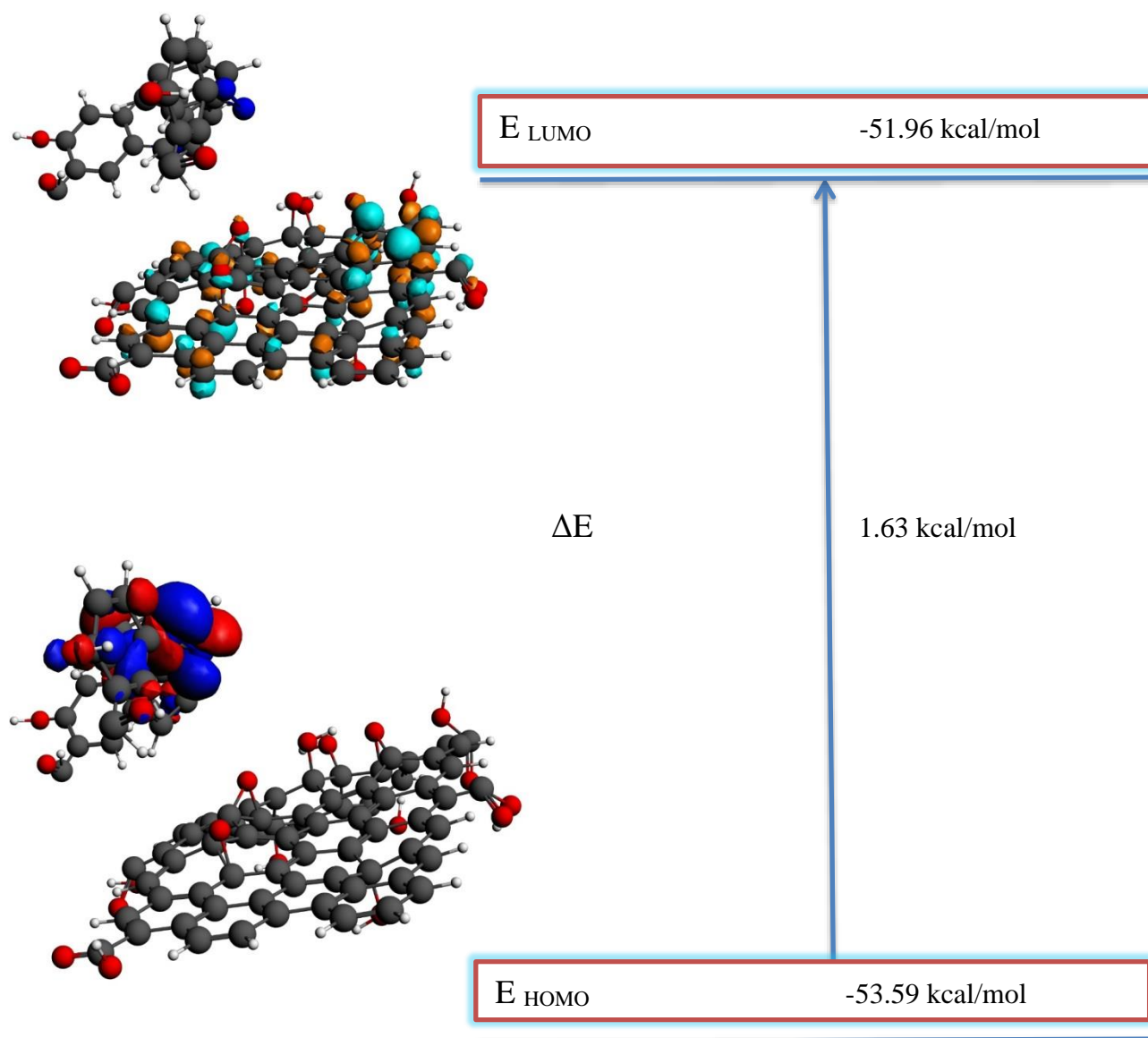
Fig 4.12: HOMO-LUMO gap of (HT 1-4) adsorbed on the surface of Graphene Oxide (GO)

| E $_{LUMO}$ | -81.54 kcal/mol |

ΔE   1.06 kcal/mol

| E $_{HOMO}$ | -82.60 kcal/mol |
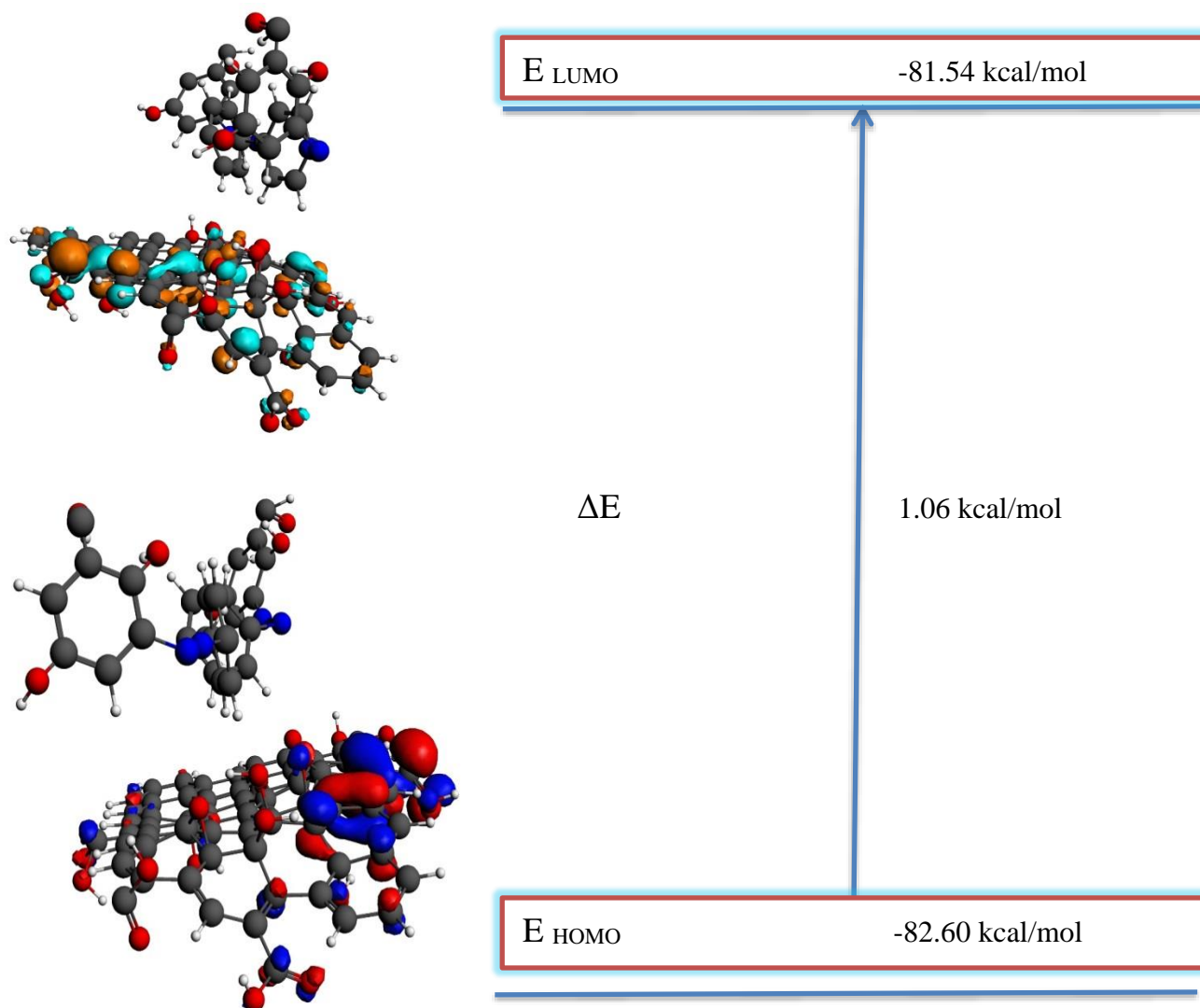
Fig 4.13: HOMO-LUMO gap of (HT 1-4) adsorbed on the surface of Graphene Oxide (GO)

Table 4.5 Electronic Interactions after adsorption $\Delta E = E_{HOMO} - E_{LUMO}$ in kcal/mol

S.NO	Distance (Å)	E_{HOMO} kcal/mol	E_{LUMO} kcal/mol	$\Delta E = E_{HOMO} - E_{LUMO}$ kcal/mol
(HT 1-1)+GO	3.5(296,297A_A)	-134.45	-133.67	0.77
(HT 1-2)+GO	3.5(317,318A_A)	-74.73	-72.91	1.82
(HT 1-3)+GO	3.5(313,314A_A)	-111.61	-103.65	7.95
(HT 1-4)+GO	3.5(324,325A_A)	-53.59	-51.96	1.63
(HT 1-5)+GO	3.5(314,315A_A)	-82.60	-81.54	1.06

4.3.2 Kinetics and Thermodynamics of adsorption

Azo dyes adsorbed at the distance of 3.5 Å on the surface of the Graphene Oxide nano-sheet for finding the kinetic and thermodynamic parameters. A negative value of interaction energy (ΔG) represented the favored adsorption whereas positive value indicated the theoretically unfavored interaction of azo dyes with the GO surface (Table 4.6). It has been observed that closer distance provided theoretically unfavored adsorption due to electronic cloud overlapping and repulsion at distance shorter than 3.5 Å and abrupt rise in energy was attributed to electron-electron and nucleus-nucleus repulsion of azo dyes and GO. 3.5 Å was observed best suited for physisorption and Vander Waal's interactions. Adsorption constant K_{ad} is calculated from free energy data as shown in (Table 5.3). Enthalpic and entropic contributions of azo dyes (HT 1-1), (HT 1-2), (HT 1-3), (HT 1-4), and (HT 1-5) after adsorption were developed and thermodynamic data indicated the fact that the adsorbate-adsorbents interactions moved towards spontaneity with lesser heat contents.

According to the Boltzmann's entropy formula developed the relationship between the number of microstates and entropy is

$$S = k \ln W \qquad\qquad 4.3$$

Where k = Boltzmann's constant and W is the number of microstates

Microstate (W) indicated more randomness at equilibrium distance and hence contributed to the larger value of ΔS at equilibrium[87].

Computational data revealed that adsorption constant values for azo dye (HT 1-4) highest due to its coupler *i.e.,* 2- hydroxybenzaldehyde. (HT 1-4) coupler formed strong intermolecular interaction between -OH, -CHO coupler groups with -COC group of graphene oxide nanoparticles was observed. (HT 1-3) has the lowest affinity of adsorption on the surface of Graphene Oxide as compared to other azo dyes (HT 1-1), (HT 1-2), (HT 1-4) and (HT 1-5) because of 1-naphthaldehyde is very stable, conjugated and aromatic coupler. (HT 1-3) coupler formed intramolecular interaction hence its adsorption rate was lesser than other azo dyes. Free energy also revealed that azo dye (HT 1-4) has more negative value *i.e.,* more spontaneous and (HT 1-3) has lesser negative values as compared to other dyes *i.e.,* less spontaneous as shown in Table 4.6. Dimethyl-sulfoxide (DMSO) dominating the interaction of azo dye (HT 1-4) with graphene oxide so its scaling factor was included.

Table 4.6 Kinetics and Thermodynamic parameter after adsorption at 3.5Å distance between azo dyes (HT 1-1), (HT 1-2), (HT 1-3), (HT 1-4), (HT 1-5) and Graphene Oxide at temperature 298K

S.NO	Enthalpy $Cv \times dT$	Entropy	Heat Capacity	Gibbs Free Energy	K_{ad}
	ΔH kJ/mol	ΔS kJ/mol-K	C_v kJ/mol-K	ΔG kJ/mol	(M^{-1})
(HT 1-1)+GO	182.13	0.83	0.61	-57.37	1.13×10^{10}
(HT 1-2)+GO	164.7	0.79	0.55	-52.41	1.51×10^{09}
(HT 1-3)+GO	55.73	0.5	0.184	-30.72	2.42×10^{05}
(HT 1-4)+GO	187.02	0.83	0.64	-58.69	1.93×10^{10}
(HT 1-5)+GO	125.89	0.66	0.42	-51.01	8.74×10^{08}

Computational results also revealed that water molecules can be passed through Graphene Oxide (GO) but azo-dyes cannot pass from the Graphene Oxide (GO) as shown in (Fig 4.14).
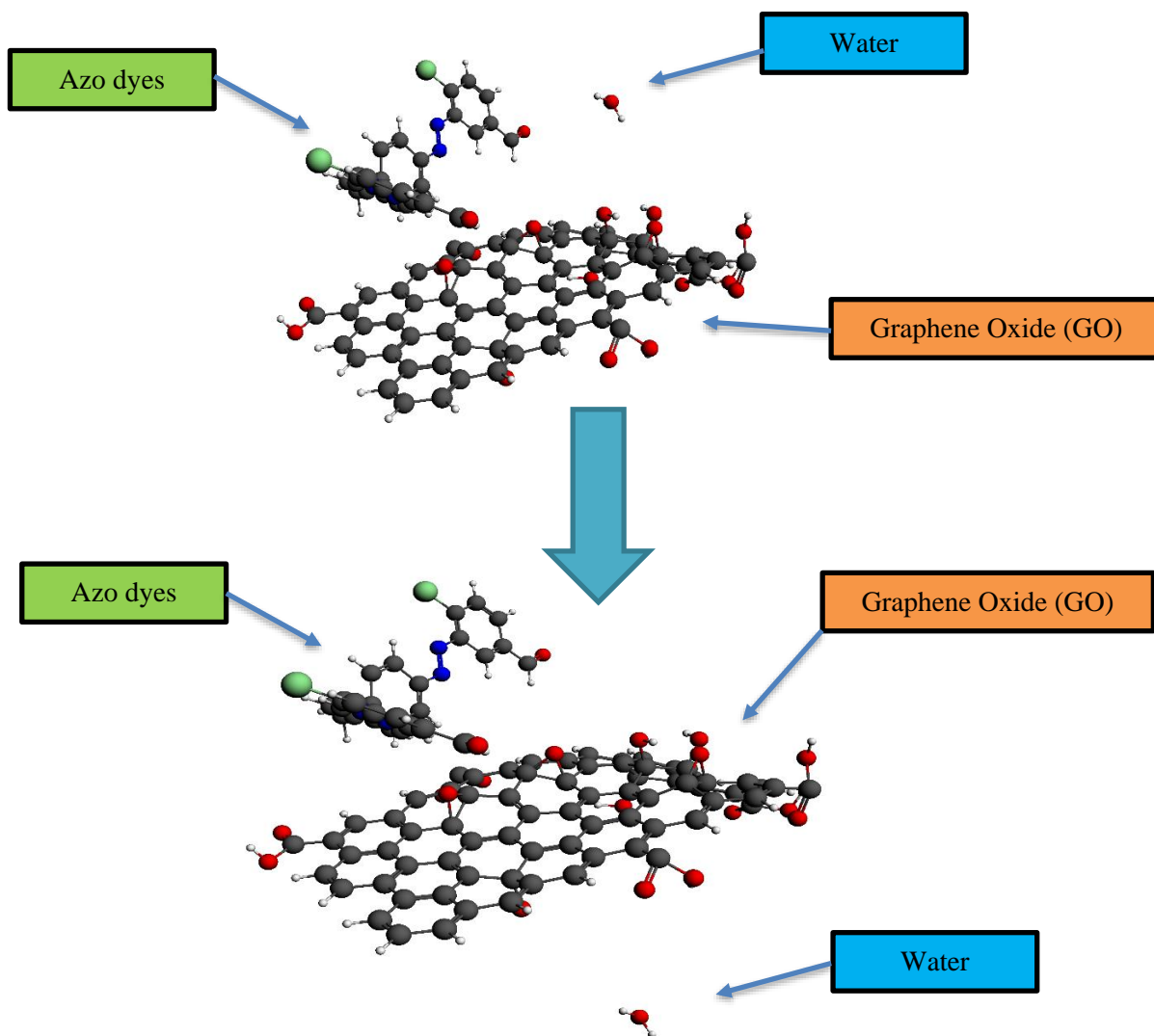
Fig 4.14: Passage of water molecules through graphene hexagone leaving behind large sized azo-dyes; Graphene is acting as molecular sieve

4.4 Comparison of Experimental and Computational results

Comparative analysis of experimental results and computational findings revealed nature of adsorption between azo-dyes and Graphene Oxide (GO) was found physisorption. Adsorption constant (K_{ad}) values are significantly high for (HT 1-4) in both processes because of functional group present on its coupler formed strong intermolecular interaction with the epoxide group of graphene oxide nanoparticle. Free energy values are negative for all azo dyes (HT 1-1), (HT 1-2), (HT 1-3), (HT 1-4), and (HT 1-5). Azo dye (HT 1-3) showed lowest adsorption constant (K_{ad}) value calculated from both experimental and computational results because its highly conjugated coupler formed pi-pi intramolecular interaction in both approaches as shown in Table 4.7 below

Table 4.7 Comparison of Gibb's free energy (ΔG) and adsorption constant calculated from experimental and computational results

Azo Dye	Computational Results		Experimental Results	
S.NO	K_{ad} (M^{-1})	Gibbs Free Energy (ΔG) kJ/mol	K_L (M^{-1})	Gibbs Free Energy (ΔG) kJ/mol
(HT 1-1) + GO	1.13×10^{10}	-57.37	1.94×10^{9}	-52.99
(HT 1-2) + GO	1.53×10^{9}	-52.41	1.37×10^{9}	-52.13
(HT 1-3) + GO	2.42×10^{5}	-30.72	7.08×10^{8}	-50.49
(HT 1-4) + GO	1.93×10^{10}	-58.69	3.76×10^{9}	-54.62
(HT 1-5) + GO	8.74×10^{8}	-51.01	1.55×10^{9}	-52.43

Chapter 5

Conclusions and Future Perspectives

Chapter 5

CONCLUSIONS AND FUTURE PERSPECTIVES

5.1 Conclusions

Five novel azo dyes and Graphene Oxide (GO) are synthesized by means of the coupling process and exfoliation method. The nanoparticle was synthesized by Modified Hummer's method and characterization was done by FT-IR and UV-Vis spectroscopy. The structure of all dyes and Graphene Oxide was created in .xyz input file format by means of ADF2018.105.

Five novel azo dyes were probed for their adsorption mechanism through Graphene Oxide molecular sieve employing both experimental UV-Vis Spectroscopic and computational quantum chemical (DFT) approaches.

In experimental effect of dosage, contact time, and Langmuir adsorption isotherms were studied while in computational electronic, kinetic and thermodynamic investigation was carried out to explore the adsorption behavior of (HT 1-1), (HT 1-2), (HT 1-3), (HT 1-4), and (HT 1-5) on Graphene Oxide using quantum mechanical *i.e.,* density functional theory (DFT) studies to validate experimental results. Electronic parameters included the E_{HOMO} and E_{LUMO} to identify the region of high and low electron density for electron transfer mechanism between azo dyes and adsorbent whereas kinetic parameters included adsorption constant (K_{ad}) indicative of the strength of bonding between azo dyes and adsorbent whereas thermodynamic descriptor involved adsorption energy, enthalpic and entropic contribution associated with internal energy change during adsorption process by means of experimental and computational. Simulation results revealed that water molecules can pass through graphene molecular sieve leaving large sized azo-dyes molecule behind thus azo-dye contaminated industrial water into purified water.

The adsorption study revealed a significant result of contribution towards the adsorption of azo dyes and wider application towards the textile, marble, and pharmaceutical industries. In computational study, 3.5-Å distance placed between each dye and epoxide –COC of Graphene Oxide and -C=C of azo dyes; whereas Langmuir adsorption isotherm used for finding the adsorption constant (K_{ad}) and free energy

(ΔG). Results revealed that a smaller HOMO-LUMO gap always has maximum adsorption constant values and greater spontaneity of heterogeneous processes.

We also predict that we can study the adsorption process by means of computational and experimental.

5.2 Future Perspectives

Azo dyes being used in textile industry and released as waste in water, impose deteriorating effect on environment by affecting the aquatic organism, forest, and humans through drinking water. Current research will be helpful for the removal of these dyes the azo dyes from wastewater by adsorption on the surface of Graphene Oxide (GO) nano-sheet. The foremost benefit of the current research in the future will be the treatment of water, and the recycling to be used as molecular sieves effectively. Research included various experimental and computational methods to be used for the removal of a large variety of molecular partially insoluble waste in water. At present, the one of the serious challenge encountered over the world is the clean drinking water scarcity which can be achieved using modern heterogeneous adsorption procedures.

References

[1]   A. Popat, P. V Nidheesh, T. S. A. Singh, and M. S. Kumar, "Mixed industrial wastewater treatment by combined electrochemical advanced oxidation and biological processes," *ECSN*, p. 124419, 2019.

[2]   C. R. Holkar, A. J. Jadhav, D. V Pinjari, N. M. Mahamuni, and A. B. Pandit, "A critical review on textile wastewater treatments : Possible approaches," *J. Environ. Manage.*, vol. 182, pp. 351–366, 2016.

[3]   A. Fiorentino *et al.*, "Science of the Total Environment Impact of industrial wastewater on the dynamics of antibiotic resistance genes in a full-scale urban wastewater treatment plant," *Sci. Total Environ.*, vol. 646, pp. 1204–1210, 2019.

[4]   E. H. Ezechi, S. R. M. Kutty, K. Muda, and A. Yaqub, "Journal of Water Process Engineering A comparative evaluation of an integrated hybrid bioreactor treating industrial wastewater," *J. Water Process Eng.*, vol. 31, no. December 2018, p. 100805, 2019.

[5]   J. K. Ahmed and M. Ahmaruzzaman, "Journal of Water Process Engineering A review on potential usage of industrial waste materials for binding heavy metal ions from aqueous solutions," *J. Water Process Eng.*, vol. 10, pp. 39–47, 2016.

[6]   E. Khosla, S. Kaur, and P. N. Dave, "Ionic dye adsorption by zinc oxide nanoparticles," no. May 2015, pp. 37–41.

[7]   A. Nautiyal and S. R. Shukla, "Journal of Water Process Engineering Silver nanoparticles catalyzed reductive decolorization of spent dye bath containing acid dye and its reuse in dyeing," *J. Water Process Eng.*, vol. 22, no. September 2017, pp. 276–285, 2018.

[8]   L. Espinar-barranco *et al.*, "AC SC," *Dye. Pigment.*, 2019.

[9]   C. Zhang, B. Chen, Y. Bai, and J. Xie, "A new functionalized reduced graphene oxide adsorbent for removing heavy metal ions in water via coordination and ion exchange," *Sep. Sci. Technol.*, vol. 00, no. 00, pp. 1–10, 2018.

[10]   B. Zhang, R. Hu, D. Sun, T. Wu, and Y. Li, "Fabrication of chitosan / magnetite- graphene oxide composites as a novel bioadsorbent for adsorption and detoxification of Cr (VI) from aqueous solution," no. October, pp. 1–12, 2018.

[11]   M. Wei, H. Chai, Y. Cao, and D. Jia, "Sulfonated Graphene Oxide as an Adsorbent for Removal of Pb2+ and Methylene blue," *J. Colloid Interface Sci.*, 2018.

[12]   I. Chemistry, "Graphene oxide and its application as adsorbent to wastewater treatment George Z. Kyzas, Eleni A.

Deliyanni * and Kostas A. Matis."

[13]   N. P. Raval, P. U. Shah, and N. K. Shah, "Malachite green '' a cationic dye ''' and its removal from aqueous solution by adsorption," *Appl. Water Sci.*, 2016.

[14]   F. Ge, H. Ye, M. Li, and B. Zhao, "Efficient removal of cationic dyes from aqueous solution by polymer-modified magnetic nanoparticles," *Chem. Eng. J.*, vol. 198–199, pp. 11–17, 2012.

[15]   E. K. Aziz, R. Abdelmajid, L. M. Rachid, and E. Haddad, "Adsorptive removal of anionic dye from aqueous solutions using powdered and calcined vegetables wastes as low-cost adsorbent," *Arab J. Basic Appl. Sci.*, vol. 0, no. 0, pp. 1–10, 2018.

[16]   O. A. Attallah, M. A. Al-ghobashy, and M. Y. Salem, "solution with magnetite / pectin and magnetite / isotherm and mechanism analysis †," *RSC Adv.*, vol. 6, pp. 11461–11480, 2016.

[17]   E. Alver and Ü. Metin, "Anionic dye removal from aqueous solutions using modified zeolite : Adsorption kinetics and isotherm studies," vol. 202, pp. 59–67, 2012.

[18]   H. Li, Y. Wang, Y. Wang, H. Wang, K. Sun, and Z. Lu, "Bacterial degradation of anthraquinone dyes *," vol. 20, no. 6, pp. 528–540, 2019.

[19]   P. Taylor, J. M. Fanchiang, and D. H. Tseng, "Decolorization and transformation of anthraquinone dye Reactive Blue 19 by ozonation," no. August 2013, pp. 37–41, 2009.

[20]   M. F. Siddiqui, S. Andleeb, N. Ali, and P. B. Ghumro, "Biotreatment of anthraquinone dye Drimarene Blue K 2 RL," vol. 4, no. 1, pp. 45–50, 2010.

[21]   S. M. Oxide, "Effective Dye Degradation by Graphene Oxide Supported Manganese Oxide," pp. 11–13, 2019.

[22]   N. Nanoparticles, S. L. Foster, K. Estoque, M. Voecks, N. Rentz, and L. F. Greenlee, "Removal of Synthetic Azo Dye Using Bimetallic," vol. 2019, 2019.

[23]   N. C. Fernandes *et al.*, "Removal of azo dye using Fenton and Fenton-like processes: Evaluation of process factors by Box–Behnken design and ecotoxicity tests," *Chem. Biol. Interact.*, 2018.

[24]   M. Chen, W. Ding, J. Wang, and G. Diao, "Removal of Azo Dyes from Water by Combined Techniques of Adsorption , Desorption , and Electrolysis Based on a Supramolecular Sorbent," 2013.

[25]   A. Chen, B. Yang, and Y. Zhou, "Effects of azo dye on simultaneous biological removal of azo dye and nutrients in wastewater," pp. 1–9, 2018.

[26] P. Semeraro *et al.*, "Removal of an Azo Textile Dye from Wastewater by Polymers Removal of an Azo Textile Dye from Wastewater by Cyclodextrin-Epichlorohydrin Polymers."

[27] R. Article, "Azo Dye Removal Technologies," vol. 5, no. 1, pp. 1–6, 2018.

[28] B. Zhang, R. Shi, W. Duan, Z. Luo, Z. Lu, and S. Cui, "Direct comparison between chemisorption and physisorption : a study of poly (ethylene glycol) by," *RSC Adv.*, vol. 7, no. Di, pp. 33883–33889, 2017.

[29] F. Costanzo, P. L. Silvestrelli, and F. Ancilotto, "Physisorption , Diffusion , and Chemisorption Pathways of H 2 Molecule on Graphene and on (2 , 2) Carbon Nanotube by First Principles Calculations," 2012.

[30] E. G. Z. Palizban, "Comparisons of azo dye adsorptions onto activated carbon and silicon carbide nanoparticles loaded on activated carbon," *Int. J. Environ. Sci. Technol.*, vol. 13, no. 2, pp. 501–512, 2016.

[31] C. Djilani, R. Zaghdoudi, F. Djazi, and B. Bouchekima, "Adsorption of dyes on activated carbon prepared from apricot stones and commercial activated carbon," vol. 000, pp. 1–10, 2015.

[32] K. Narcisse, Y. Augustin, and K. Benjamin, "Investigation of dye adsorption onto activated carbon from the shells fruit of Macor e Gon e," vol. 156, pp. 10–14, 2015.

[33] S. I. Raj, A. Jaiswal, and I. Uddin, "dye adsorbent," pp. 11212–11219, 2019.

[34] R. S. De Farias *et al.*, "Adsorption of congo red dye from aqueous solution onto amino-functionalized silica gel," pp. 1053–1060, 2018.

[35] A. K. Kushwaha, N. Gupta, M. C. Chattopadhyaya, and E. Chemistry, "Journal of Chemical and Pharmaceutical Research," vol. 2, no. 6, pp. 34–45, 2010.

[36] R. W. Gaikwad and S. A. Misal, "Sorption Studies of Methylene Blue on Silica Gel," vol. 1, no. 4, pp. 342–345, 2010.

[37] E. Wu *et al.*, "OPEN A Novel Preparation of Nano- Copper Chalcogenide (Cu 2 S) -based Flexible Counter Electrode," *Sci. Rep.*, no. October 2018, pp. 1–9, 2019.

[38] H. L. Nguyen, H. N. Nguyen, and H. H. Nguyen, "Nanoparticles : synthesis and applications in life science and environmental technology *," *Adv. Nat. Sci. Nanosci. Nanotechnol.*, vol. 6, no. 1, p. 15008.

[39] R. K. Sahu, S. S. Hiremath, Y. Sakka, and H. R. Ghorbani, "A review on the classification , characterisation , synthesis of nanoparticles and their application A review on the classification , characterisation , synthesis of nanoparticles and their application," 2017.

[40]   M. B. Wayu, M. J. Pannell, N. Labban, S. Case, J. A. Pollock, and M. C. Leopold, "Functionalized carbon nanotube adsorption interfaces for electron transfer studies of galactose oxidase," *Bioelectrochemistry*, p. #pagerange#, 2018.

[41]   N. Sharma *et al.*, "Synthesis and Characterization of Graphene Oxide (GO) and Reduced Graphene Oxide (rGO) for Gas Sensing Application," vol. 1700006, pp. 1–5, 2017.

[42]   J. G. X. Gao, M. L. Q. Nie, and W. P. R. Liu, "Dye adsorption on electrochemical exfoliated graphene oxide nanosheets : pH influence , kinetics and equilibrium in aqueous solution," 2016.

[43]   B. Y. Zhu *et al.*, "Graphene and Graphene Oxide : Synthesis , Properties , and Applications," pp. 3906–3924, 2010.

[44]   D. Bitounis, H. Ali-boucetta, B. H. Hong, and D. Min, "Prospects and Challenges of Graphene in Biomedical Applications," pp. 1–11, 2013.

[45]   P. Avouris, "Graphene : Electronic and Photonic Properties and Devices," pp. 4285–4294, 2010.

[46]   J. T. Catal, S. P. Lonkar, and A. A. Abdala, "Thermodynamics & Catalysis Applications of Graphene in Catalysis Graphene Oxide (GO) Reduced Graphene Oxide," vol. 5, no. 2, 2014.

[47]   E. Preparation, L. G. O. Sheets, and T. C. Films, "Efficient Preparation of Large-Area Graphene Oxide Sheets for Transparent Conductive Films," vol. 4, no. 9, pp. 5245–5252, 2010.

[48]   Y. Qian, I. M. Ismail, and A. Stein, "graphene oxide and resol," *Carbon N. Y.*, vol. 68, pp. 221–231, 2013.

[49]   B. Konkena and S. Vasudevan, "Understanding Aqueous Dispersibility of Graphene Oxide and Reduced Graphene Oxide through p K," 2012.

[50]   M. M. Gudarzi, "Colloidal Stability of Graphene Oxide: Aggregation in Two Dimensions," 2016.

[51]   O. C. Compton *et al.*, "Tuning the Mechanical Properties of Graphene Oxide Paper and Its Associated Polymer Nanocomposites by Controlling Cooperative Intersheet Hydrogen Bonding," no. 3, pp. 2008–2019, 2019.

[52]   J. Litofsky and R. Viswanathan, "Introduction to Computational Chemistry: Teaching Hü ckel Molecular Orbital Theory Using an Excel Workbook for Matrix Diagonalization."

[53]   L. E. Johnson and T. Engel, "Curriculum," pp. 569–573, 2011.

[54]   E. C. Anota and H. Hern, "LDA approximation based analysis of the adsorption of O 3 by boron nitride sheet," vol. 273, pp. 271–273, 2011.

[55]   D. Vasi, Z. Ristanovi, I. Pašti, and S. Mentus, "Systematic DFT – GGA Study of Hydrogen Adsorption on Transition Metals 1," vol. 85, no. 13, pp. 2373–2379, 2011.

[56]   M. Mahdavian, H. Yari, B. Ramezanzadeh, G. Bahlakeh, and M. Hasani, *Immobilization of Ultraviolet Absorbers on Graphene oxide Nanosheets to be utilized as a Multifunctional Hybrid UV-blocker: A Combined Density Functional Theory and Practical Application*. 2018.

[57]   A. Molla, Y. Li, B. Mandal, S. G. Kang, S. H. Hur, and J. S. Chung, "Selective Adsorption of Organic Dyes on Graphene Oxide: Theoretical and Experimental Analysis," *Appl. Surf. Sci.*, 2018.

[58]   L. Gan *et al.*, "Graphene oxide incorporated alginate hydrogel beads for the removal of various organic dyes and bisphenol A in water," 2018.

[59]   D. Jahanshahi, B. Vahid, and J. Azamat, "Computational study on the ability of functionalized graphene nanosheet for nitrate removal from water," *Chem. Phys.*, vol. 511, pp. 20–26, Jul. 2018.

[60]   J. Azamat, A. Khataee, and F. Sadikoglu, *PT*. Elsevier B.V, 2017.

[61]   W. Konicki, M. Aleksandrzak, and E. Mijowska, "Equilibrium, kinetic and thermodynamic studies on adsorption of cationic dyes from aqueous solutions using graphene oxide," *Chem. Eng. Res. Des.*, 2017.

[62]   R. Shiralipour and A. Larki, "Ecotoxicology and Environmental Safety Pre-concentration and determination of tartrazine dye from aqueous solutions using modi fi ed cellulose nanosponges," vol. 135, pp. 2016–2018, 2017.

[63]   P. Borthakur, P. K. Boruah, N. Hussain, Y. Silla, and M. R. Das, "Specific ion effect on the surface properties of Ag/reduced graphene oxide nanocomposite and its influence on photocatalytic efficiency towards azo dye degradation," *Appl. Surf. Sci.*, vol. 423, pp. 752–761, 2017.

[64]   G. M. D. Ferreira *et al.*, "Adsorption of red azo dyes on multi-walled carbon nanotubes and activated carbon: A thermodynamic study," *Colloids Surfaces A Physicochem. Eng. Asp.*, vol. 529, no. April, pp. 531–540, 2017.

[65]   Y. Qi, M. Yang, W. Xu, S. He, and Y. Men, "Natural polysaccharides-modified graphene oxide for adsorption of organic dyes from aqueous solutions," *J. Colloid Interface Sci.*, vol. 486, pp. 84–96, 2017.

[66]   M. Y. Nassar, A. S. Amin, I. S. Ahmed, and S. Abdallah, "Journal of the Taiwan Institute of Chemical Engineers Sphere-like Mn 2 O 3 nanoparticles : Facile hydrothermal synthesis and adsorption properties," vol. 64, pp. 79–88, 2016.

[67]   M. Paszkiewicz, A. Go, A. Rajski, E. Kowal, A. Sajdak, and A. Zaleska-medynska, "The Antibacterial and

Antifungal Textile Properties Functionalized by Bimetallic Nanoparticles of Ag / Cu with Different Structures," vol. 2016, 2016.

[68] D. Robati *et al.*, "Removal of hazardous dyes-BR 12 and methyl orange using graphene oxide as an adsorbent from aqueous phase," *Chem. Eng. J.*, vol. 284, pp. 687–697, 2016.

[69] P. Banerjee, S. Sau, P. Das, and A. Mukhopadhayay, "Optimization and modelling of synthetic azo dye wastewater treatment using Graphene oxide nanoplatelets: Characterization toxicity evaluation and optimization usingArtificial Neural Network," *Ecotoxicol. Environ. Saf.*, vol. 119, pp. 47–57, 2015.

[70] P. Taylor, A. Debnath, K. Deb, K. K. Chattopadhyay, and B. Saha, "Desalination and Water Treatment Methyl orange adsorption onto simple chemical route synthesized crystalline α -Fe 2 O 3 nanoparticles : kinetic , equilibrium isotherm , and neural network modeling," no. June, pp. 37–41, 2015.

[71] Q. S. Ferreira, S. W. Silva, C. M. B. Santos, G. C. Ribeiro, L. R. Guilherme, and P. C. Morais, "Rifampicin adsorbed onto magnetite nanoparticle : SERS study and insight on the molecular arrangement and light effect," no. June, pp. 765–771, 2015.

[72] M. A. Kassem and G. O. El-sayed, "Adsorption of Tartrazine on Medical Activated Charcoal Tablets under Controlled Conditions," vol. 1, no. 1, pp. 1–7, 2014.

[73] X. Rong, F. Qiu, J. Qin, H. Zhao, J. Yan, and D. Yang, "Ac ce p d us t," *J. Ind. Eng. Chem.*, 2014.

[74] C. Klett, A. Barry, I. Balti, P. Lelli, F. Schoenstein, and N. Jouini, "Journal of Environmental Chemical Engineering Nickel doped Zinc oxide as a potential sorbent for decolorization of specific dyes , methylorange and tartrazine by adsorption process," *Elsevier*, vol. 2, no. 2, pp. 914–926, 2014.

[75] A. Fakhri, "Adsorption characteristics of graphene oxide as a solid adsorbent for aniline removal from aqueous solutions : Kinetics , thermodynamics and mechanism studies," pp. 52–57, 2017.

[76] F. Zhang, J. Lan, Y. Yang, and T. Wei, "Adsorption behavior and mechanism of methyl blue on zinc oxide nanoparticles," 2013.

[77] M. Ghaedi, F. Karimi, B. Barazesh, R. Sahraei, and A. Daneshfar, "Journal of Industrial and Engineering Chemistry Removal of Reactive Orange 12 from aqueous solutions by adsorption on tin sulfide nanoparticle loaded on activated carbon," *J. Ind. Eng. Chem.*, vol. 19, no. 3, pp. 756–763, 2013.

[78] H. Wang, Y. Shen, C. Shen, Y. Wen, and H. Li, "Enhanced adsorption of dye on magnetic Fe 3 O 4 via HCl-assisted sonication pretreatment," *DES*, vol. 284, pp. 122–127, 2012.

[79]   F. M. Machado *et al.*, "Adsorption of Reactive Red M-2BE dye from water solutions by multi-walled carbon nanotubes and activated carbon," *J. Hazard. Mater.*, vol. 192, no. 3, pp. 1122–1131, 2011.

[80]   S. M. Kanawade, "Low cost Sugarcane Bagasse Ash as an Adsorbent for Dye Removal from Dye Effluent," vol. 1, no. 4, pp. 309–318, 2010.

[81]   J. Song, X. Wang, and C. Chang, "Preparation and Characterization of Graphene Oxide," vol. 2014, 2014.

[82]   P. Taylor, S. E. Rizk, and M. M. Hamed, "Desalination and Water Treatment Batch sorption of iron complex dye , naphthol green B , from wastewater on charcoal , kaolinite , and tafla," no. February 2015, pp. 37–41, 2014.

[83]   D. C. Emeniru, J. Ikirigo, and F. Sogbara, "Perspective View on Sorption Thermodynamics : Basic Dye Uptake on Southern Nigerian Clay," vol. 13, no. 18, 2017.

[84]   L. Zhao, A. Xin, F. Liu, J. Zhang, and N. Hu, "Results in Physics Secondary bending effects in progressively damaged single-lap , single-bolt composite joints," *Results Phys.*, no. September, 2016.

[85]   M. B. Desta, "Batch Sorption Experiments : Langmuir and Freundlich Isotherm Studies for the Adsorption of Textile Metal Ions onto Teff Straw (Eragrostis tef) Agricultural Waste," vol. 2013, 2013.

[86]   E. Paquet, "Computational Methods for Ab Initio Molecular Dynamics," vol. 2018, 2018.

[87]   G. S. Girolami *et al.*, "A Brief History of Thermodynamics, As Illustrated by Books and People," 2019.